Heliyon 8 (2022) e11308

Contents lists available at ScienceDirect

Heliyon

journal homepage: www.cell.com/heliyon

Research article

Multivariate statistical and hydrochemical approaches for evaluation of groundwater quality in north Bahri city-Sudan

Musaab A.A. Mohammed [a,*], Norbert P. Szabó [a,b], Péter Szűcs [a,b]

[a] University of Miskolc, 3515 Miskolc, Hungary
[b] MTA-ME Geoengineering Research Group, University of Miskolc, Egyetemváros, Hungary

ARTICLE INFO

Keywords:
Bahri locality
Nile river
Nubian aquifer
Hierarchical cluster analysis
Principal component

ABSTRACT

Groundwater has recently been considered one of the primary sources of water supply in Sudan. However, groundwater quality is continuously degraded due to overexploitation and long-term agricultural operations. The fossilized Cretaceous Nubian sandstone is the principal aquifer in the study area. This research aims to determine the major factors influencing groundwater quality and detect the suitability of groundwater for drinking and irrigation purposes by integrating hydrochemical and multivariate statistical methods. Hydrochemical plots such as Piper, Chadha, and Durov diagrams were applied to detect the groundwater facies and hydrochemical processes controlling the groundwater quality. They indicated Ca–Mg–HCO_3 water type as a dominant groundwater facies followed by Na–HCO_3 and Na–Cl types. Gibbs plots suggested that the dissolution of the minerals is the main factor influencing the water quality. The results of the Gibbs plot were further interpreted using saturation indices (SI). The SI values indicated that aragonite, calcite, and dolomite precipitated respectively in 58.33%, 75%, and 75% of groundwater samples. Multivariate statistical analyses, including Pearson's correlation analysis, hierarchical cluster analysis (HCA), and principal component analyses (PCA), were jointly employed to identify the structure of water quality data and deduce the main factors controlling groundwater quality. The statistical analysis revealed the effect of the physical and human-induced activities as the main factors influencing groundwater chemistry. These factors are rock-water interaction, agricultural practice, and organic contamination from septic tanks. Further, the suitability of groundwater for irrigation is determined using sodium adsorption ratio (SAR) and sodium percent (Na^+%) indices. They carefully indicated that 75% of the groundwater samples in the study area are excellent for irrigation except for some sample location where the salinity hazard is stimulated by ion exchange. This integrated approach was effective in calibrating water quality assessment methodologies. The current research concluded that the implication of a groundwater quality monitoring scheme is crucial to ensure water supply sustainability in north Bahri city.

1. Introduction

Groundwater supplies freshwater for drinking and other household needs to most people worldwide (P. Li, Qian, et al., 2018). Groundwater use for domestic and agricultural reasons has undoubtedly increased its demand worldwide. However, groundwater is susceptible to contamination from both natural and artificial sources (Singh et al., 2015). Groundwater in Sudan is a fundamental source of water supply. It is a critical component of population settlement and sustainable socio-economic activities (Hassan et al., 2017). The demand for Groundwater has increased dramatically to fulfill the development plans; nevertheless, these changes have posed various issues, such as inefficient pumping, reduced dependable production, and deterioration of groundwater quality (Abdo and Salih, 2012). The primary sources of water supply in Bahri city are the Nile River and groundwater. The groundwater supplies about 52% of the total need, mainly for irrigation. The sophistication in irrigation, chemical fertilizers, and pesticides has helped sustain life for many Sudanese people. On the other hand, the widespread adoption of pesticides and chemical fertilizers damaged groundwater quality and soil permeability. Water quality degradation leads to an increase in groundwater salinity, caused mainly by natural and anthropogenic activities. Consequently, the expense of health care and irrigation is rising, while the standard of living and the agricultural economy is declining (Rishi et al., 2020). Groundwater quality is as vital

* Corresponding author.
E-mail address: musab20501@gmail.com (M.A.A. Mohammed).

https://doi.org/10.1016/j.heliyon.2022.e11308
Received 7 June 2022; Received in revised form 5 October 2022; Accepted 25 October 2022

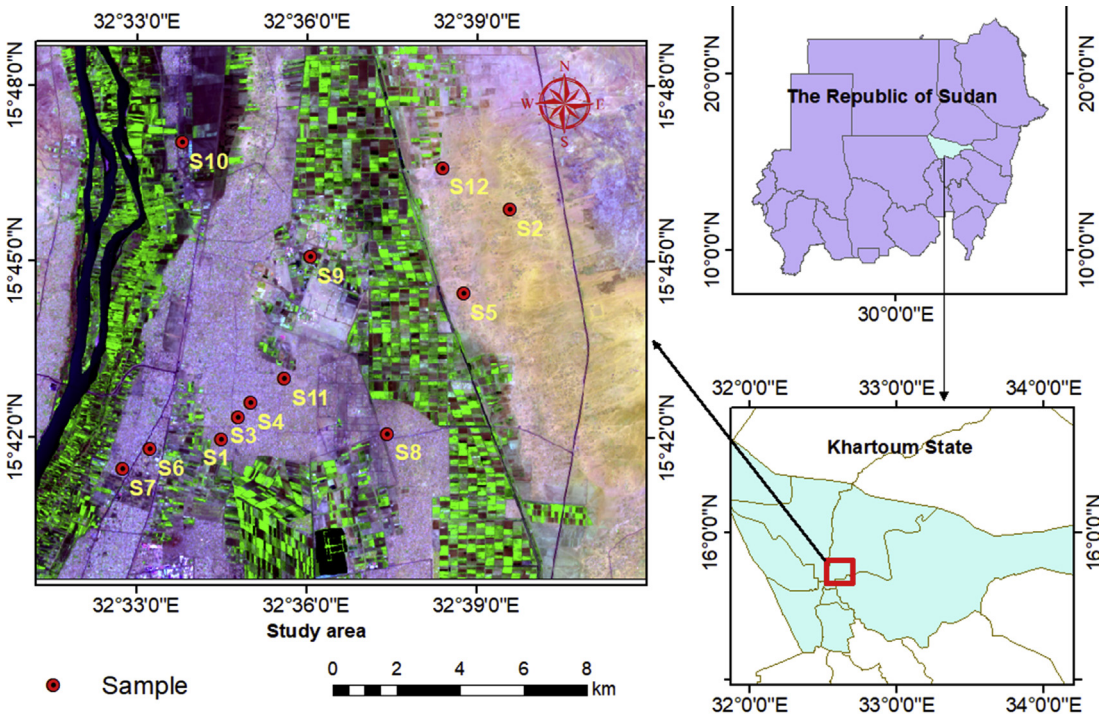

Figure 1. Location of the groundwater samples investigated by the proposed hydrogeochemical approaches.

as quantity since it determines its usefulness for drinking and irrigation. Therefore, the hydrochemical assessment of groundwater aquifers is crucial for water resource management and development. The evaluation of the groundwater offers insight into the effects of natural and human-induced disturbances on the water resources and the suitability of the groundwater for drinking and irrigation purposes.

Few studies regarding water quality were conducted in Bahri city. For example (Elkrail et al., 2003); assessed the spatial distribution of the major chemical parameters. Their study indicated that the ion concentration appreciably increases with increasing distance from the surface water systems. Alsidig and Al-Hagaz, 2019 evidenced that the groundwater in Bahri city ranges from generally acceptable to good for domestic uses. Kudoda and Abdalla, 2015 indicated that three factors are affecting groundwater quality in Khartoum state. These factors are mineral dissolution and weathering, carbonate system, and anthropogenic effect. Abdo and Salih, 2012 assessed the drinking water quality in north Bahri city. They reported that 55% of the investigated water samples are affected by coliform bacteria. Abdelsalam et al., 2016 discussed the factors retard the groundwater consumption in Khartoum state. They noted that the groundwater quality is affected by faulty groundwater well design and seepage of contamination from septic tanks and latrines. However, almost all the explored studies rely on identifying the chemical parameters and comparing them to a given quality standard without providing due account to delineating the contamination sources. The factors affecting the groundwater quality and hydrochemical properties of the groundwater have been widely documented in recent years, for example (Adimalla, 2019; Ben Brahim et al., 2021; Ismail et al., 2021; Kaur et al., 2019; Khalid, 2019; P. Li, Qian, et al., 2018; Rafaâ Trigui et al., 2021; Sunkari et al., 2020; Zhang et al., 2021). These investigations aided in developing hydrochemical studies, making them a dependent tool in water quality control and prediction. Multivariate statistical approaches are utilized to efficiently analyze and appraise the physicochemical properties of groundwater (Bhimanagouda et al., 2020; Dlamini and Demlie, 2020; Duan et al., 2022; Elumalai et al., 2020; Enyegue A Nyam et al., 2020; Ibrahim et al., 2019; Lu et al., 2012; Osiakwan et al., 2021; Ren et al., 2021; Ziani et al., 2021). Multivariate statistical

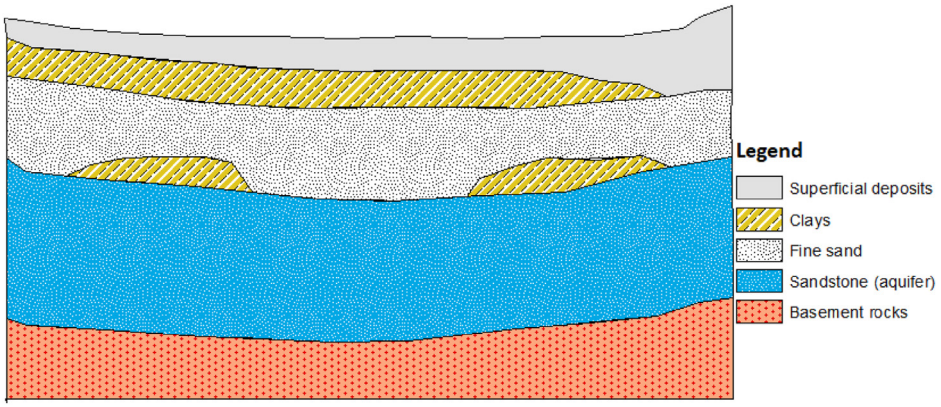

Figure 2. The simplified hydrogeological cross-section from the southwestern to north-eastern part.

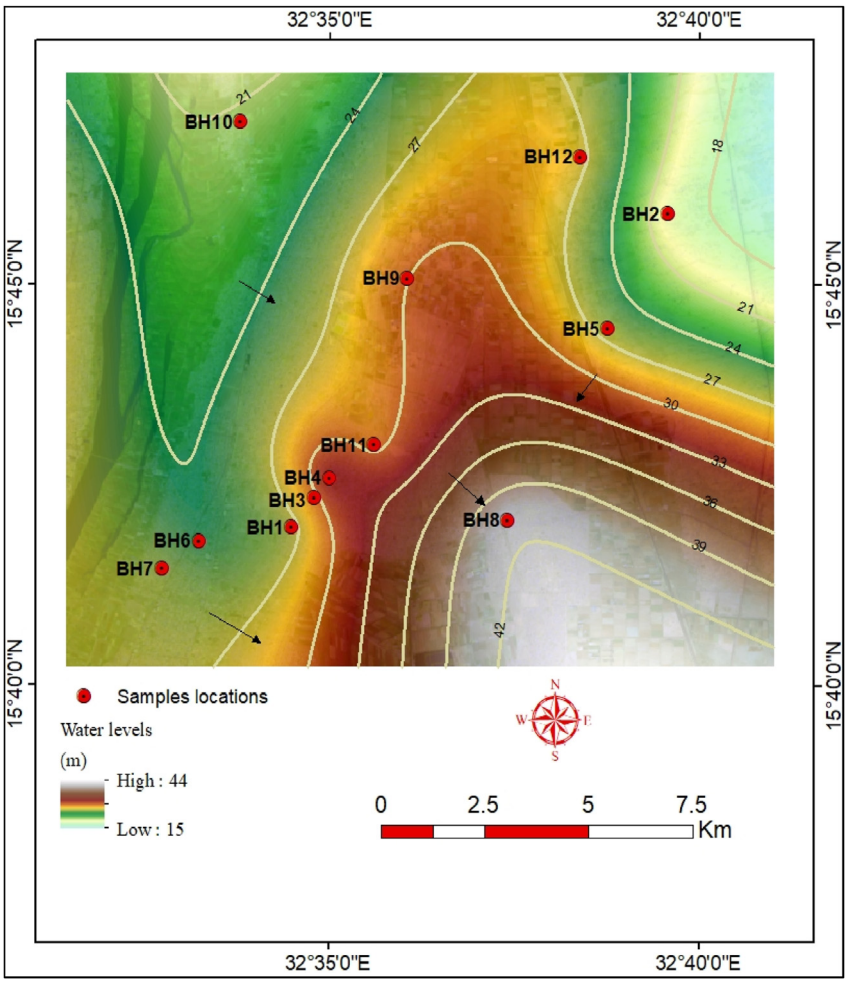

Figure 3. Potentiometric surface map showing the diverse direction of groundwater flow in the study area.

techniques are used to acquire information about similarities between groundwater samples, the variables that determine groundwater quality, and the hidden components that affect the data structure (Bhakar and Singh, 2019; Gulgundi and Shetty, 2018; Sheikhi et al., 2021). Hydrochemical and multivariate statistical analyses effectively understand the aquifer's characteristics and behavior concerning groundwater contamination (Ma et al., 2014; Masoud and Ali, 2020). The specific properties and the key groups of groundwater quality can be conveniently presented and categorized using multivariate statistical methods (Abdelaziz et al., 2020; Lu et al., 2012). Irrigation indices such as sodium adsorption ration and sodium percent have been widely used for assessing groundwater quality for irrigation purposes (Asadi et al., 2020; Kaur et al., 2021; P. Li et al., 2019; Masoud and Ali, 2020; Othman et al., 2019; Wilcox, 1948). Such indices are particularly useful for informing the public and relevant agencies about the quality of groundwater for different water management scenarios.

The study area is densely populated agricultural land with few water sources. On the other hand, anthropogenic pollution, namely agricultural activities, produce both point sources and diffuse contamination observed in scattered localities. This study aims to assess groundwater quality for irrigation and household uses in the north Bahri locality using hydrochemical and multivariate statistics methods. This integrated approach is efficient in detecting the chemical characteristics of groundwater and determining the vertical and horizontal variation in the groundwater facies. This study is considered the most comprehensive study to assess groundwater quality in the central Sudan hydrogeologic system. It can be used as a guide for future groundwater quality studies in similar regions in Sudan.

2. Materials and methods

2.1. The study area

The research area is in north Bahri city, Khartoum state, Sudan. It covers about 250 km^2, and the Nile River confines it from the west (Figure 1). The area is located in the northern part of the Savanna belt, which is characterized by a hot climate. The average annual rainfall ranges from 100 to 200 mm/year. Topographically, the study area is a flat peneplain. These plains rise gradually from ground 340 m (MSL) in the middle of the site to 600 m towards the eastern part. About 80% of the population lives along the Nile River, and the density of the population drops rapidly away from the Nile. The study area consists of three geological units; the Precambrian basement rocks are the oldest in the study area. They are composed of gneisses, schists, and granites, which appear on the surface outside the region, primarily on the northern and eastern sides. The Precambrian rocks are overlain unconformably by the Nubian formation of the Cretaceous age, which is considered the prime aquifer (Awad, 1994; Kheiralla, 1966; Saeed, 1974; Whiteman, 1971). This formation consists of conglomerates, sandstone, and mudstone. They are intruded on by basaltic rocks. The recent deposits encountered in the study area include windblown sands and alluvium wadi deposits (Figure 2). Groundwater is found in the Nubian formation's poorly cemented sandstone strata in confined to semiconfined conditions. This is due to silts and clays in thick to thin aquitards and aquicludes (Abdelsalam et al., 2016). Nubian sandstone forms two aquifers (Farah et al., 1997). An upper aquifer of thicknesses ranges from 10 to 300 m, and a lower one with a thickness of more than 400 m. The groundwater

Table 1. The results of the analyzed physicochemical parameters in this research.

sample number	pH	E.C (μS/cm)	TDS (mg/L)	TA (mg/L)	T.H (mg/L)	Cl^- (mg/L)	F^- (mg/L)	SO_4^{-2} (mg/L)	NH_3^- (mg/L)	NO_3^- (mg/L)	Ca^{+2} (mg/L)	Mg^{+2} (mg/L)	Na^+ (mg/L)	HCO_3^- (mg/L)
1	7.3	601.5	330.8	226	234	23	0.24	52	0.21	3.2	35.2	35	37.6	226
2	7.5	588	411.6	396.5	230.6	11.36	0.2	37	0.354	13.64	48.6	26.5	88.4	396.5
3	7.4	590	354	248	208	8	0.2	28	0.1	1.2	40.3	25.4	37.2	248
4	7.2	585	322	250	200	12	0.25	27.9	0.11	3	38.4	25	46.8	250
5	7.9	1500	1050	414.8	380	193.12	1.23	320.5	0.3	0.07	16	82.6	332.8	414.8
6	7.4	485	339.5	414.8	254	12.78	BDL	98	BDL	9.24	56	27.7	37.01	414.8
7	8.3	417	292	243.8	186	120.7	BDL	4	0.5	0.1	32	25.8	17.6	231.8
8	8	357	214.4	142	134	9	0.62	14	0.32	5.3	24	17.8	19.8	142
9	7.8	858	600.6	396	190	82.5	0.35	86	0.2	5.72	66.4	5.8	124.32	378.2
10	7.4	518	362.6	281.6	185	23.856	0.59	23	0.03	6.1	38.4	22.3	45.9	281.6
11	7.5	650	375	276	232	18	0.35	41	0.14	1.4	52.8	24	46.5	276
12	7.7	929	694.4	304.8	260	91.5	0.1	152	0.39	7.48	57.6	28.2	123	292.8

levels vary from10 to 15 m near the Nile River and reach up to 45 m in the eastern and northern parts of the study area. The drainage system is dominated by the Nile River and local systems of ephemeral streams (e.g., Wadis and Khors), which trend mostly east-west. The flow of groundwater shows diverse directions but mostly flows from the Nile River to the east and southern part of the area (Figure 3). In the research area, there are two main groups of the recharged groundwater that can be identified depending on their source and expected time of recharging: Nilotic and Meteoric waters. Nilotic groundwater infiltrated from the Niles after the middle Holocene and retained in upper and lower aquifers within a 12-kilometer radius from the Nile River. Meteoric paleo groundwater that recharged between the Pleistocene and middle Holocene and exists in the regions outside the Nile influence. The recent recharge from rainfall is minimal, with the exception of regions close to ephemeral streams, wadis, and depressions (Farah et al., 2000).

2.2. Groundwater sampling

In 2018, a total of 12 samples is taken during the post-monsoon season. The groundwater samples were taken from bore wells installed in the north Bahri city that were privately owned and ranged in depth from 100 to 150 m. The geographical distribution of the samples is shown in Figure 1. Groundwater samples were collected based on the well's accessibility and reliability, and the collected samples were kept in previously cleaned plastic bottles. Groundwater samples were analyzed for physicochemical parameters by Khartoum State Water Corporation (KSWC). These parameters are total alkalinity (TA), total hardness (TH), calcium (Ca^{+2}), sodium (Na^+), magnesium (Mg^{+2}), chloride (Cl^-), nitrate (NO_3^-), sulfate (SO_4^{-2}), bicarbonate (HCO_3^-) fluorides (F^-), and Ammonia (NH_3^-). Electrical conductivity (EC), total dissolved solids (TDS), and pH were measured using a multi-parameter portable instrument immediately after the sample collection. The accuracy of the physicochemical analysis was examined by the electrical balance (EB) between the cations and anions using the formula (equation (1)) suggested by (Appelo and Postma, 2005)

$$(\mathrm{EB}\%) = \frac{\sum \text{cations} - \sum \text{anions}}{\sum \text{cations} + \sum \text{anions}} \times 100 \quad (1)$$

All anions and cations were in milliequivalents per liter. In this research, the EB% was within ±5%, which indicates good accuracy.

2.3. Hydrochemical and statistical analysis

Hydrochemical tests were performed to define the groundwater facies, detect the geographical distribution of chemical parameters, and demonstrate the physiochemical mechanisms that influence groundwater chemistry using different hydrochemical plots (Chadha, 1999; Durov, 1948; Gibbs, 1970; Piper, 1944).

Multivariate statistical techniques were employed to investigate the primary factors influencing the quality of groundwater in the north Bahri locality. The statistical methods such as correlation, cluster, and principal component analyses are useful techniques for understanding the sources of groundwater contamination (Wu et al., 2020). First, the correlation between the physiochemical parameters is applied to study the degree of associations between them and detect the role of each parameter in the overall quality. The correlation analysis aids in monitoring the chemical parameters and understanding the interrelation between the various water quality variables (Rishi et al., 2020). Pearson correlation coefficient (r) is utilized in this study. It can be computed using Eq. (2) as

$$r = \frac{\sum_i^n (x_i - \bar{x})(y_i - \bar{y})}{\sqrt{\sum_i^n (x_i - \bar{x})^2} \sqrt{\sum_i^n (y_i - \bar{y})^2}} \quad (2)$$

where n represent the values of the variables x and y, and $\bar{x}$ and $\bar{y}$ symbolize the means of these values.

Secondly, hierarchical cluster analysis (HCA) is performed to categorized the groundwater samples and their ions according to their chemical characteristics. It organizes the items into clusters according to a predetermined selection criterion, with each variable being comparable to the others in each cluster. Thus generated clusters exhibit both high internal homogeneity and substantial interclass variability (Daughney et al., 2012; Kaur et al., 2020). The most popular technique is hierarchical clustering, which provides inherent similarity correlations

Table 2. The simple statistics of the analyzed parameters.

Parameter	Units	Mean	Minimum	Maximum	WHO standard (Edition, 2011) (Edition, 2011)
pH	-	7.61	7.2	8.3	8.5
EC	μS/cm	673.2	357.3	1500	1500
TDS	mg/L	445.6	214.4	1050	1000
TH	mg/L	224.5	134	380	500
Cl^-	mg/L	50.5	8	193.1	250
F^-	mg/L	0.34	0	1.23	1
SO_4^{-2}	mg/L	73.6	4	320.5	250
NH_3^-	mg/L	0.23	0	0.5	3
NO_3^-	mg/L	4.7	0.07	13.64	50
Ca^{+2}	mg/L	42	16	66.4	200
Mg^{+2}	mg/L	28.9	5.8	82.6	150
Na^+	mg/L	79.7	17.6	332.8	200
HCO_3^-	mg/L	296	142	414.8	350

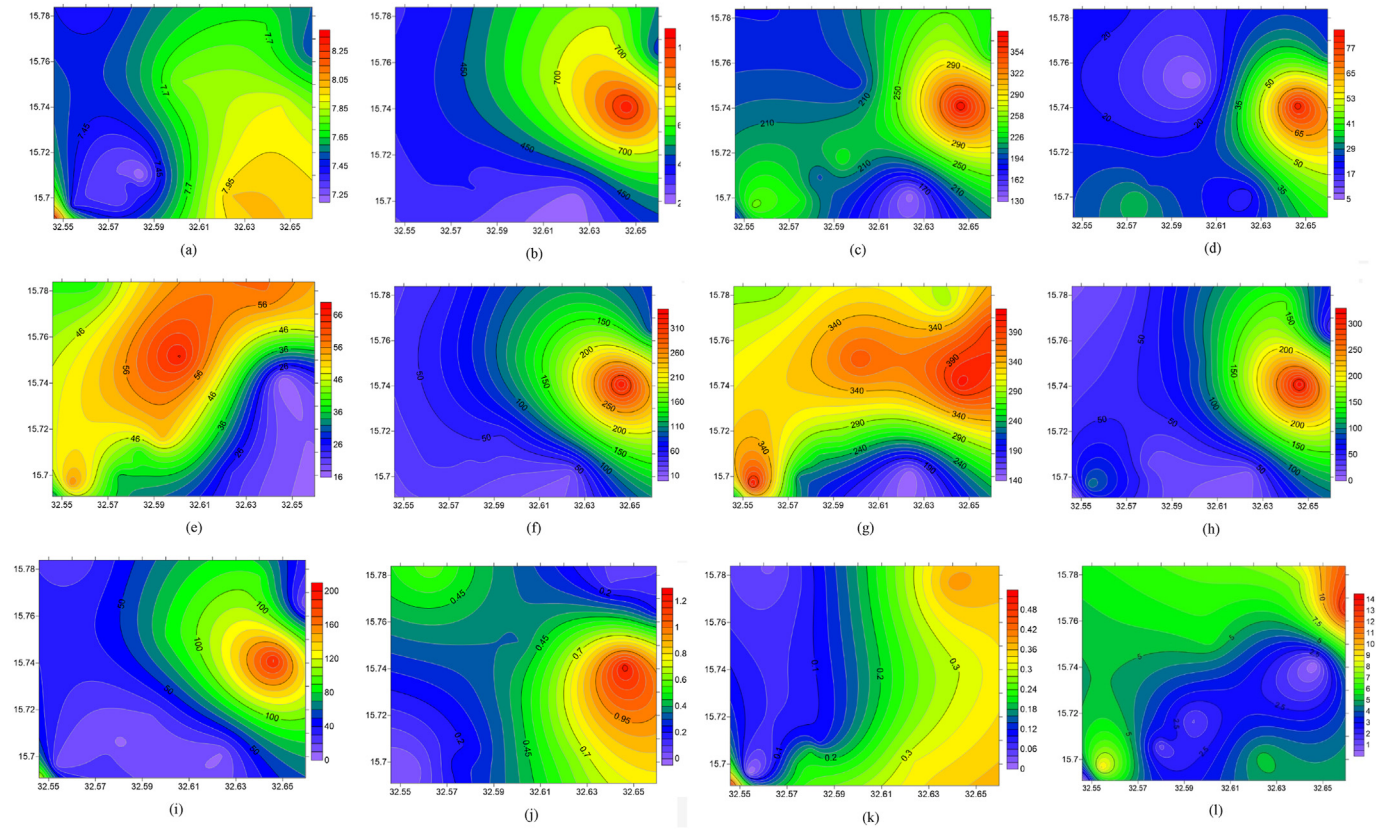

Figure 4. The geographical distribution of the chemical and physical parameters in study area (a) pH, (b) total dissolve solid, (c) total hardness, (d) magnesium, (e) calcium, (f) sodium, (g) bicarbonate, (h) sulfate, (i) chloride, (j) fluoride, (k) ammonia, (l) nitrate.

between any variable and the complete collection of data (Shrestha and Kazama, 2007). The result of the cluster analysis is visualized in dendrograms. The dendrogram reduces the complexity of the original data and offers a graphical representation of clusters and their proximity.

Finally, principal components (PCs) were obtained through principal component analysis (PCA) to detect the major components controlling the quality of groundwater in the study area. PCA is employed to reduce the dimensionality of the data for analyzing the interrelationships between a wide range of variables and explaining their common underlying factors (Kumar et al., 2011). The degree of connection between variables and their effect on the analyzed samples can be determined using PCA (Bhimanagouda et al., 2020). Extraction of the PCs, which are linear combinations of the initial variables, is the primary feature of PCA (Wu et al., 2014). The variances extracted from the PCs are called eigenvalues. The remaining variables determine how much of the residual variability (Behera and Das, 2018). The PCs (Ψ) are expressed using Eq. (3)

$$\psi = w_{i1}x_1 + w_{i2}x_2 + \cdots + w_{ip}x_p \tag{3}$$

where p is the total number of variables, i is the component number, which varies from 1 to p, w is the component loading, and x is the original variable.

2.4. Irrigation indices

Sodium adsorption ratio (SAR) and sodium percent (Na^+%) were employed to assess the suitability of groundwater for irrigation. The quality of irrigation water directly affects plant growth, which may cause a decline in crop production (P. Li et al., 2019). Therefore, using high-quality water for irrigation is crucial for agricultural development. The most generally used metric to evaluate irrigation water is SAR, which is a proportional balance of Na^+ ions to Ca^{2+} and Mg^{2+} ions in the water sample. The following formula (Eq. (4)) can be used to estimate SAR

$$SAR = \frac{Na^+}{\left\{\frac{Ca^{+2}+Mg^{+2}}{2}\right\}^{\frac{1}{2}}} \tag{4}$$

where Na^+, Ca^{+2}, and Mg^{+2} are in meq/L. On the SAR basis, water is classified into four categories: excellent category where SAR <10, in a good category SAR range from 10 to 18, doubtful is between 18 and 26, and SAR >26 for unsuitable water.

Na^+ % is one of the frequently used indices to determine the suitability of groundwater for irrigation purposes (Wilcox, 1948). Crop growth is affected by an excessive Na^+ concentration since it impacts the permeability of the soil (Todd and Mays, 2004). Na^+% is computed using eq. (5)

$$Na^+\% = \frac{Na^+}{Ca^{+2} + Mg^{+2} + Na^+ + K^+} \tag{5}$$

where all the ion concentrations are expressed in meq/L). According to Na^+%, water is classified to excellent (less than 20%), good (20–40 %), permissible (40–60 %), doubtful (60–80 %), and unsuitable (more than 80 %) (Khodapanah et al., 2009).

3. Results and discussion

3.1. General hydrochemistry

In this research, 14 physiochemical parameters are used to evaluate the groundwater quality in north Bahri city. The result of the hydrochemical analysis is shown in Table 1. The descriptive statistics such as

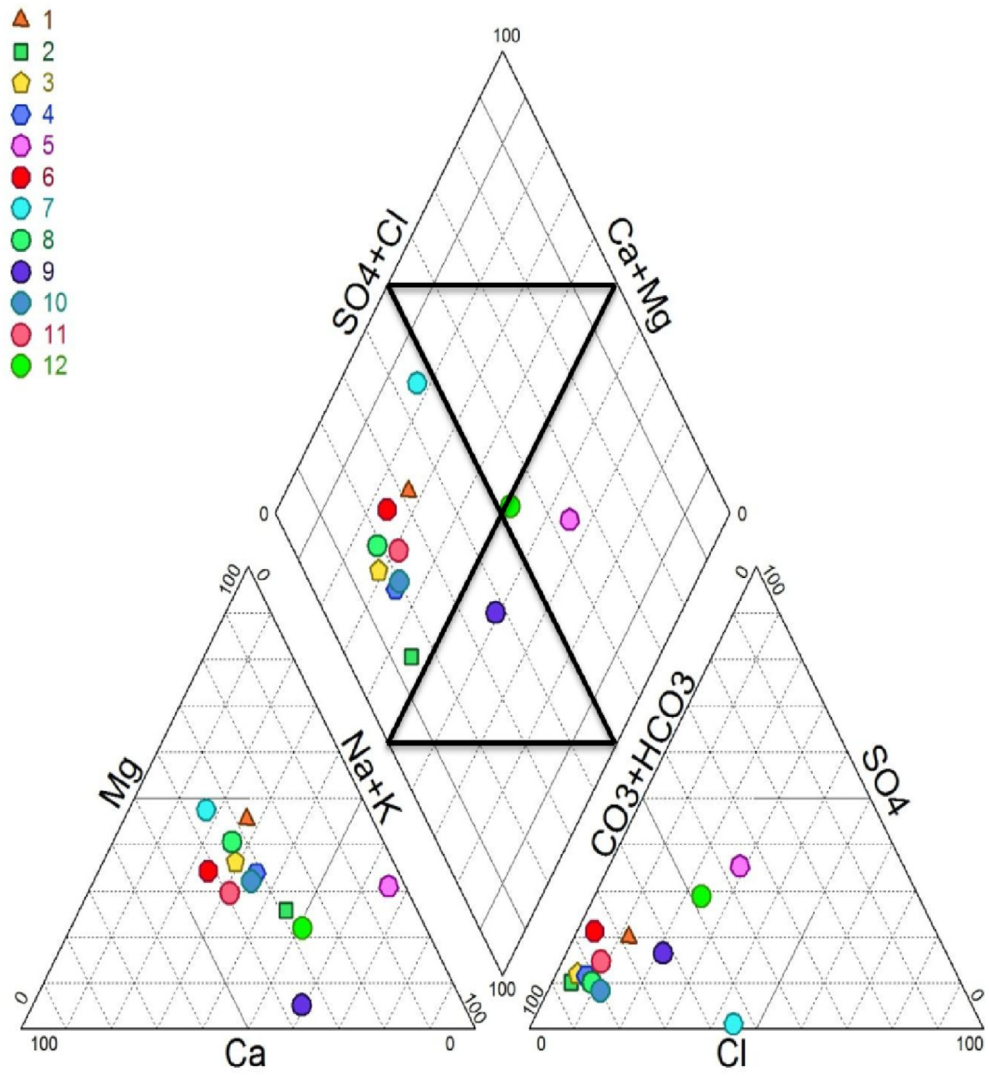

Figure 5. (a) Piper diagram of the study.

mean, minimum, and maximum for the analyzed parameters are given in Table 2 to reveal the deviation of the Physiochemical parameters from the permissible concentration limits prescribed by the World Health Organization (WHO) (Edition, 2011). Almost all the parameters are within the acceptable range prescribed by WHO. In this study, the analyzed physicochemical parameters are EC, TDS, TH, pH, Na^{+}, Ca^{+2} Mg^{+2}, Cl^{-}, SO_4^{-2}, NO_3^{-}, F^{-}, HCO_3^{-}, and NH_3^{-}. These parameters are subject to alteration depending on the surrounding environment (P. Li et al., 2016). The pH of the groundwater samples is between 7.2 and 8.3, indicating a neutral to alkaline water type. The spatial distribution of pH (Figure 4a) revealed the highest values in the southeastern part and the lowest values in the southwestern part of the study area. The EC of groundwater samples varies between 357.3 and 1500 μS/cm. Almost all the samples show EC values less than 1500 μS/cm. EC of the groundwater is directly related to the dissolved solids. The most important indicator of the overall mineral concentration in groundwater is TDS. In this study, TDS ranges from 214.4 to 1050 mg/L. The highest record is observed in the east, while the lowest is in the western part (Figure 4b). The rock-water interaction is the possible reason for the variation in the total dissolved solids. TH concentrations are below the WHO standard (Edition, 2011) and range from 134 to 380. TH of the groundwater is connected to the presence of Ca^{+2} and Mg^{+2} (Hailu et al., 2019). The content of Mg^{+2} fluctuates between 5.8 and 82.6 mg/L. Dolomite dissolution and silicate weathering are two common sources of Mg^{+2}. Since TH is mainly controlled by Mg^{+2}, therefor, the geographical variation of TH (Figure 4c) and Mg^{+2} (Figure 4d) shows a similar trend. The calcium concentration in the groundwater samples ranges from 16 to 66.4 mg/L. The highest Ca^{+2} concentration (66.4) is found in location 9 in the central part of the study area (Figure 4e). Calcium may have come via the dissolution of carbonates. In groundwater chemistry, Na^{+} is the most critical ion. Its concentration in the investigated area gradually rises from west to east (Figure 4f). Site 5 in the eastern part of the research area has the highest concentration (332.8 mg/L), while location 7 has the lowest (17.6 mg/L). Silicate weathering and halite dissolution might explain the high concentration of Na^{+} (Hem, 1985). The concentration of the HCO_3^{-} varies between 142 and 414.8 mg/L. The major anion in the research region is HCO_3^{-}. Locations 5 and 7 have the highest concentration. The areal distribution of HCO_3^{-} is shown in Figure 4g. Calcite and dolomite dissolution or ion exchange are the sources of HCO_3^{-}. The HCO_3^{-} level rises in concordance with the mineral content. The concentration of SO_4^{-2} in groundwater ranges from 4 to 320.5 mg/L and gradually increases from the west to the eastern part of the study area (Figure 4, h). It might result from soil leaching or groundwater discharge (Yidana et al., 2018). Cl^{-} concentrations range from 8 to 193.12 mg/L Cl^{-}. The highest concentration is detected in sample 5, while the lowest is recorded in sample 3. The geographical distribution of Cl^{-} is shown in Figure 4i. The maximum concentration of F− is 1.23 mg/L which is considered a high value According to WHO (Edition, 2011). The highest NH_3^{-} concentration

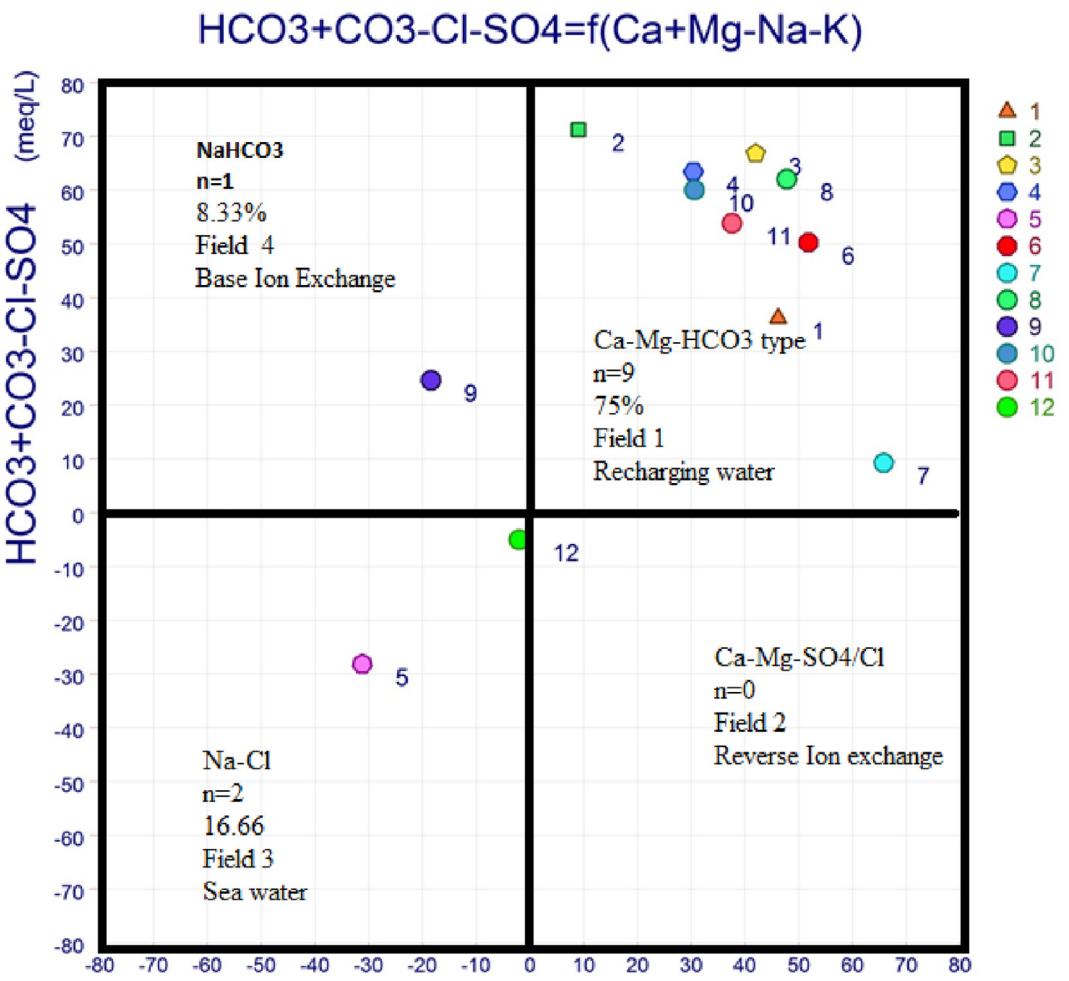

Figure 6. Chadha diagram showing the water facies in the study area.

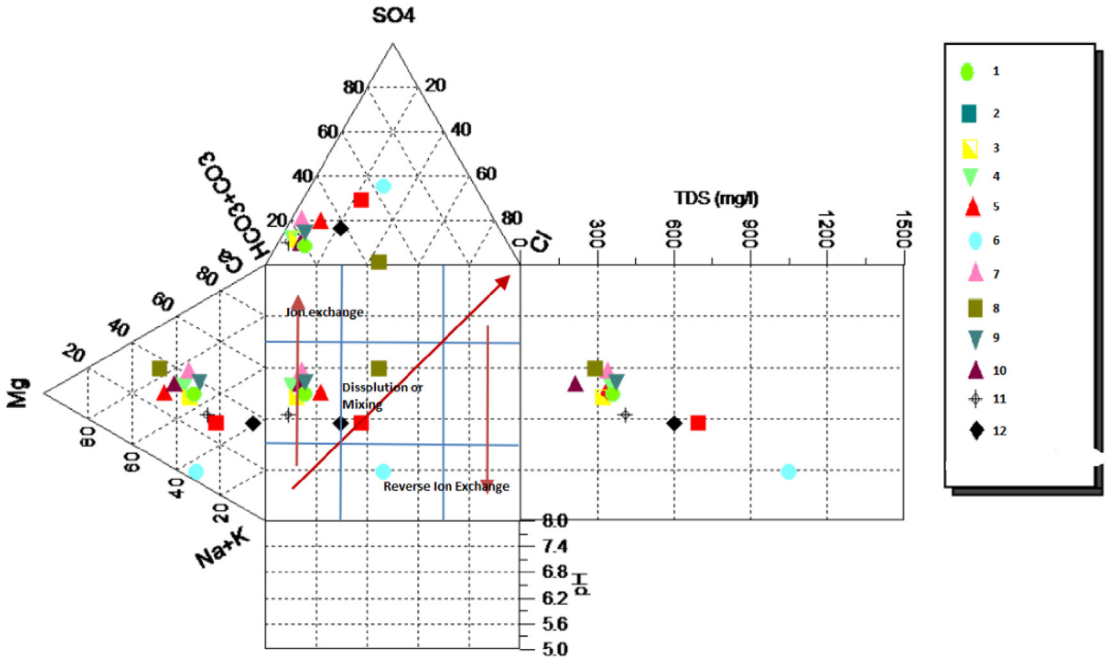

Figure 7. Durov diagram showing the dominant chemical processes affecting groundwater chemistry.

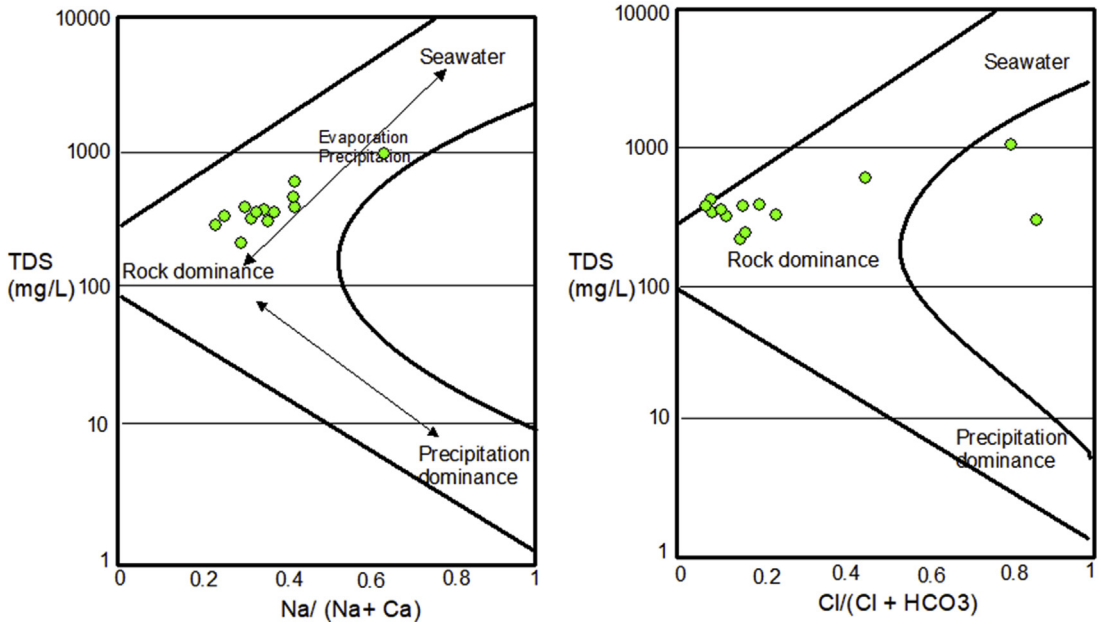

Figure 8. Gibb's plot shows the impact of rock weathering, evaporation, and precipitation on the groundwater samples.

is 0.5 mg/L and recorded in sample 7. The spatial distribution of F^- and NH_3^- is illustrated in Figure 4j and 4k, respectively. The concentration of NO_3^- ranges from 0.07 to 13.64 mg/L. The maximum concentration is recorded in sample 2, while the minimum is observed in sample 5. The spatial variation is given in Figure 4l. The essential source of NO_3^- is agricultural activities. In the majority of the samples, the order of cation dominance is $Na^+ > Ca^{+2} > Mg^{+2}$. This sequence indicates that the interaction with geological formations would have contributed the most to the hydrochemistry. The concentration of the anions in groundwater samples is allocated as $HCO_3^- > SO_4^{-2} > Cl^-$. Almost all parameters except calcium and bicarbonate increase from the east to the west part of the area, indicating that the groundwater well's recharge is coming from the Nile River. The behaviors of Ca^{+2} and HCO_3^- ions reflect the chemical composition of the Nile River water.

3.2. Hydrochemical facies

Hydrogeochemical plots such as Piper (1944), Chadha (1999), and Durov (1948) diagrams are used to appraise the water chemistry in the study area. The graphical representation helps in visualizing groundwater quality status and gives a conclusion on the groundwater facies and the processes controlling the groundwater quality. In Piper diagram, the proportion of milliequivalent concentrations for the major cations (Na^+, Mg^{+2}, and Ca^{+2}) and anions (SO_4^{-2}, HCO_3^-, and Cl^-) are displayed in two triangle fields, which are then projected onto the center diamond in a multi-dimensional shape. In the Piper diagram, the top of the diamond is associated with water high in $Ca^{+2} + Mg^{+2}$ and $Cl^- + SO_4^{-2}$, which indicates permanent hardness. The samples projected in the left corner are rich in Ca^{+2}, $Mg^{+2,}$ and HCO_3^-. It is the region of temporary hardness. Alkali bicarbonate (Na^+ and HCO_3^-) water type is projected in the lower part of the diamond shape. Saline water (Na^+ and $Cl^- + SO_4^{2-}$) is always plotted in the right part of the diamond. The result of Piper trilinear diagram is shown in Figure 5. The plotted cations indicate the dominance of Ca^{2+} and Mg and in the anion plot, HCO_3^- is dominant. Most groundwater samples (75%) fall in Ca–Mg– HCO_3 water type which is mainly influenced by the recharged water from the Nile River or perhaps caused by rock-water interaction associated with intermediate EC values. Also, the dissolution of dolomite and calcite may cause this water type. About 8.33% of the samples represent the Na–HCO_3 type. This type is likely formed as a result of the cation exchange process as it removes Ca^{+2} and Mg^{+2} and incorporates Na^+ into groundwater. Na–Cl water type dominates 16.66% of the samples. Na–Cl water type might be produced by the mixing of fresh water with saline water (Adams et al., 2001) or by reverse ion exchange (Yadav et al., 2018). The concentration of sodium increases from recharge to discharge area while the bicarbonate, on the other hand, decreases. This can be visualized as the cation exchange stimulated along the flow path.

Chadha diagram is a modified version of Piper diagram (Chadha, 1999). Groundwater cations and anions were determined at the same time step. As a result, the water chemistry data were shown as percentile difference between HCO_3–($SO_4^{-2} + Cl^-$) and ($Ca^{+2} + Mg^{+2}$)–($Na^+ + K^+$) concentrations in meq\L. Chadha diagram reveals the association between cations and anions of groundwater (Rafique et al., 2015). Four different types of water facies may be identified using the Chadha diagram: Ca–Mg–HCO_3, Na–HCO_3, Ca–Mg–SO4/Cl, and Na–Cl. Consequently, four hydrochemical processes result in the production of these water facies (Figure 6). Field 1 depicts the Ca–Mg–HCO_3 water type. This type reflects the influence of weathering and recharging processes on the groundwater. 75% of the water samples in the research area are projected in this field. Ca–Mg–SO_4/Cl water type plotted in field 2 and indicates reverse ion exchange activities and no samples is plotted in this field. Field 3 shows the NaCl water type, indicating that evaporation and mixing with saltwater have influenced water samples in this field. This zone contains 16.66 % of the water samples. The water type of Na–HCO_3 is shown in Field 4. This class contributes 8.33 % to the total hydrochemical facies.

Durov diagram (1948) has been used to indicate the hydrochemical processes controlling groundwater chemistry. Durov diagram is a plot that combines two triangles and a central rectangular shape in which the milliequivalent percentage of cations against anions is projected (Figure 7). Most of the groundwater samples with TDS less than 500 mg/L are located in the field of ion exchange, whereas samples with TDS higher than 500 mg/l are located in the dissolution and mixing zone. Durov diagram helped in the interpretation of Piper and Chadha diagrams. It showed that most of the samples are plotted in dissolution and ion exchange regions. According to (Lloyd and Heathcote, 1985), the mixing of groundwater with newly recharged water with no noticeable major anion or cation can explain this pattern.

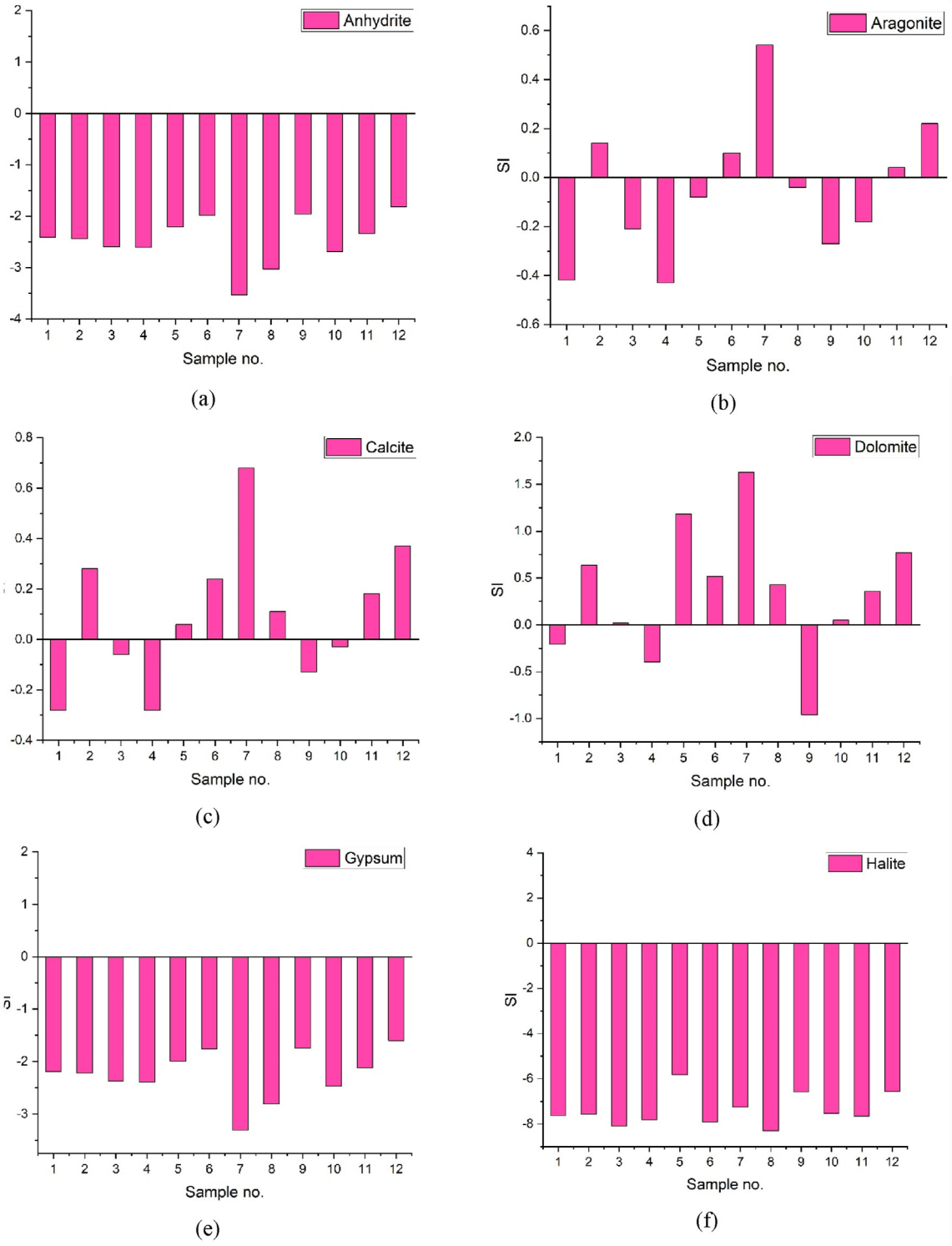

Figure 9. Saturation indices for (a) anhydrite (b) aragonite (d) calcite (c) dolomite (e) Gypsum (f) halite.

3.3. Saturation index

Gibbs diagrams are frequently used to understand how natural activities affect groundwater chemistry. In this study, the influence of several mechanisms, such as weathering of rocks, precipitation, and evaporation, was detected using Gibbs (1970) scatter plot. The ratio of $Cl^{-}/(Cl^{-} + HCO_3^{-})$ and $(Na^{+}/Na^{+} + Ca^{+2})$ is projected versus TDS concentration (Figure 8). Except for two samples that occurred in the evaporation and precipitation zone, the $Na^{+}/(Na^{+} + Ca^{+2})$ versus TDS plot revealed that the majority of the groundwater samples were affected by rock-water interaction. Chemical weathering, dissolution of carbonate minerals, and ion exchange are the main component affecting the rock-water interaction process (Boateng et al., 2016). Mineral dissolution is likely the primary natural mechanism influencing the primary salts in

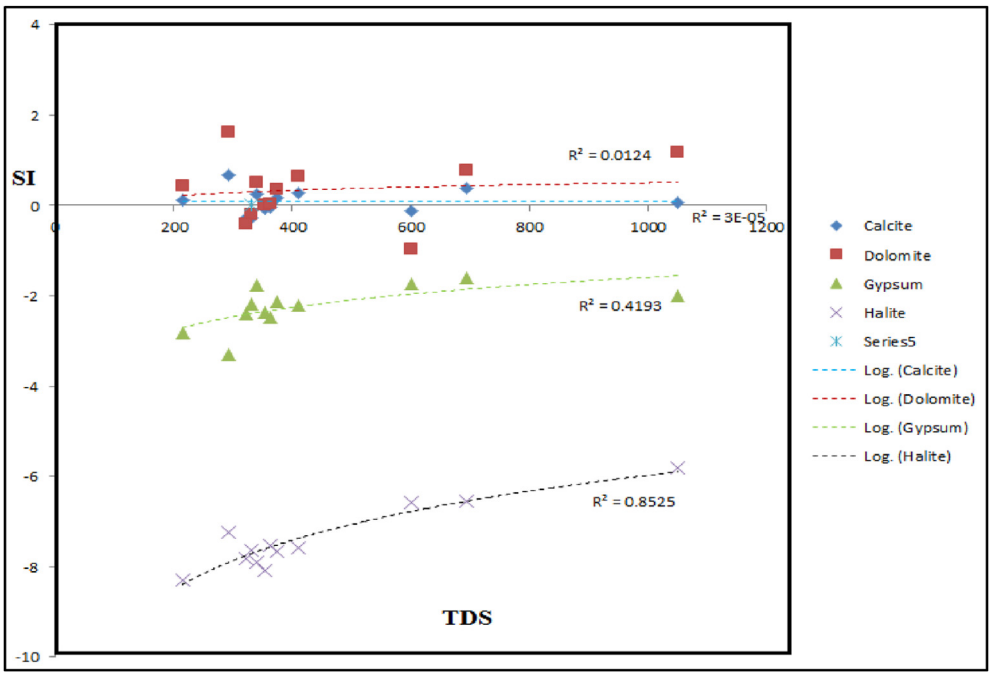

Figure 10. Correlation of TDS with saturation indices of calcite, dolomite, gypsum, and halite.

groundwater. TDS with $Cl^-/(Cl^- + HCO_3^-)$plot confirmed that those two samples of shallow depth which were affected by evaporation are also influenced by saline water intrusion. This shows that shallow aquifers in dry and semi-arid regions often experience higher rates of evaporation than deeper subterranean water sources. (Li et al., 2018b). Accordingly, it is clear that significant rock weathering and minimal evaporation together influence groundwater chemistry in the research area. To evaluate the product of the rock-water interaction, the saturation indices (SI) for major minerals such as gypsum, aragonite, dolomite, anhydrite, halite, and calcite were calculated. The calculation results are illustrated in Figure 9. The SI values of aragonite, calcite, and dolomite are higher than zero in 41.6%, 58.3%, and 75% of groundwater samples, respectively (Figure 9b, c, and d). It means the precipitation of these minerals in the majority of the groundwater samples. In contrast, the SI values of gypsum, anhydrite, and halite for all groundwater samples are less than zero (Figure 9a, e and f), indicating that groundwater might dissolve these minerals along the flow path. Groundwater in the recharge zones is unsaturated in gypsum, anhydrite, halite, aragonite, dolomite, and

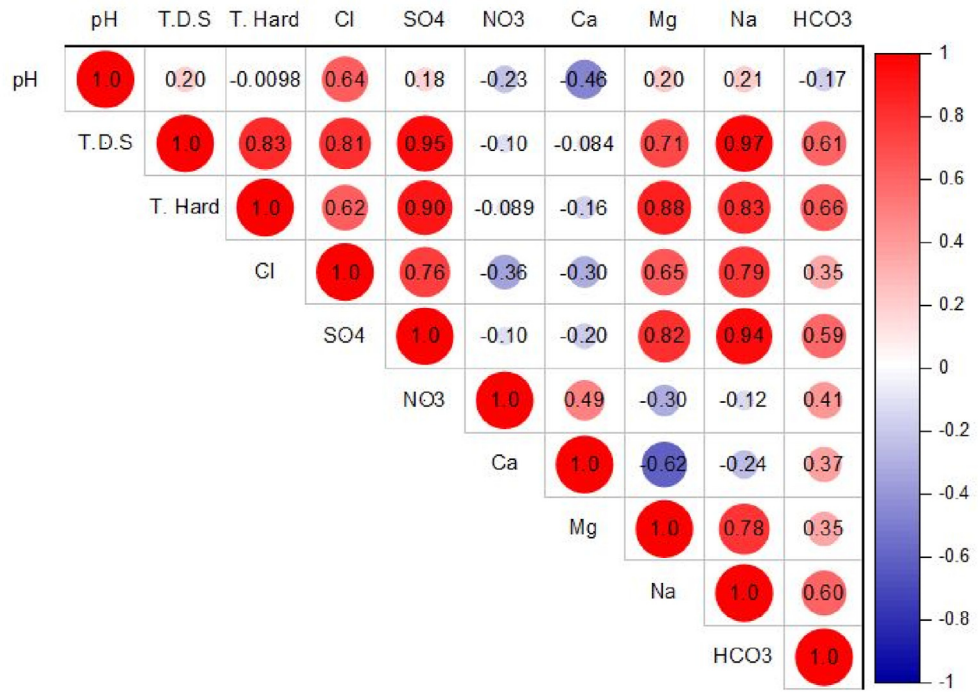

Figure 11. Pearson correlation matrix between major parameters.

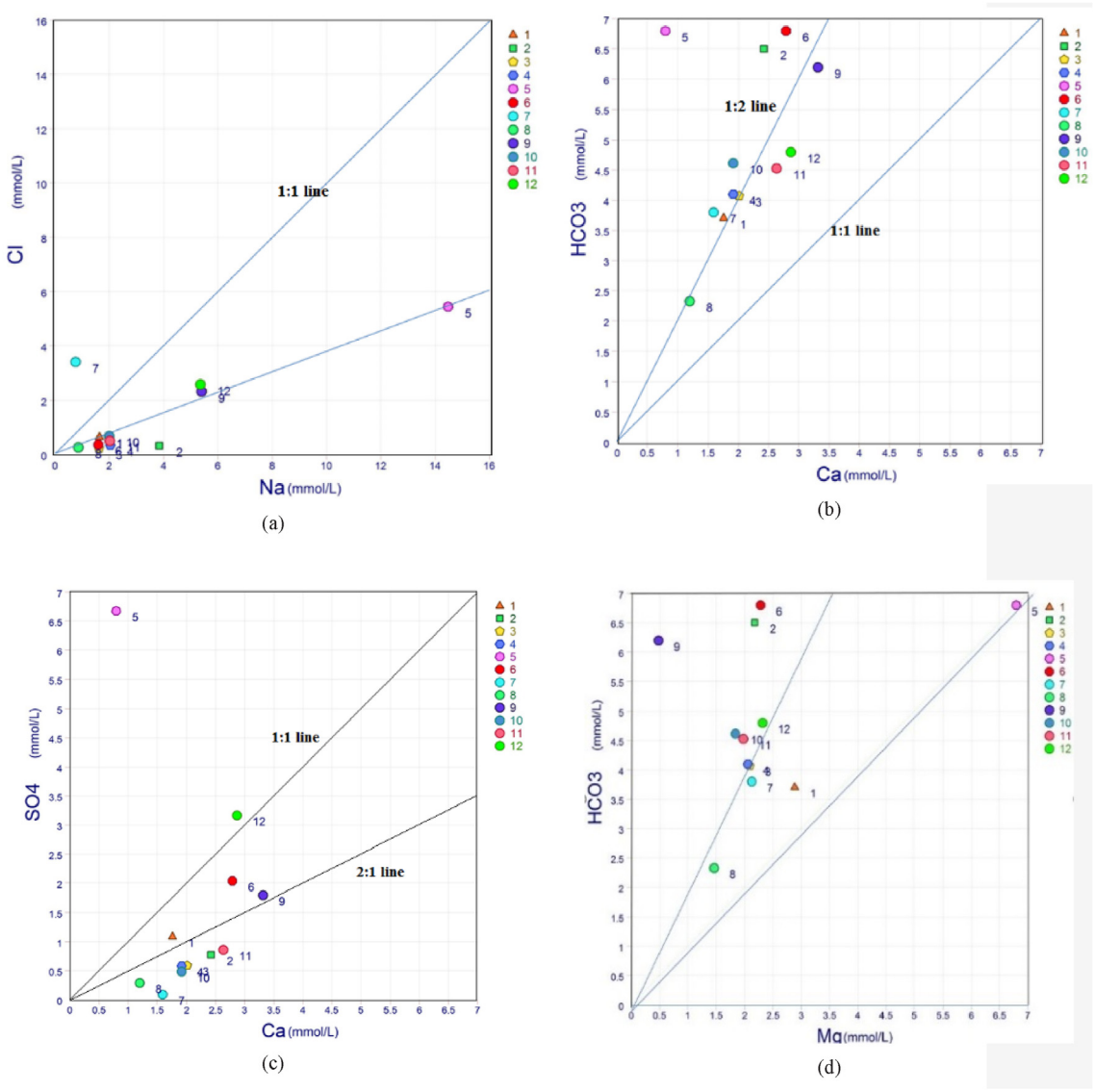

Figure 12. Correlation and regression between dominant cations and anions (a) Na^+ and Cl^-, (b) Ca^{+2} and HCO_3^- (c) Ca^{+2} and SO_4^{-2} (d) Mg^{+2} and HCO_3^-.

calcite since the contact period between the rocks and groundwater is limited. In discharge zones, groundwater achieves equilibrium with these minerals as many water-rock interactions occur. As a result of gradual mineral dissolution from recharge to discharge zones, the TDS in groundwater will rise along the groundwater flow path. The SI values of calcite and dolomite range from −0.28 to 0.68 and −0.96 to 1.63, respectively, suggesting no substantial connections between them and TDS. Therefore, Calcite and dolomite do not dissolve further along the flow path (Figure 10). On the other hand, gypsum and halite are associated with SI values less than zero and a significant positive relationship with TDS, suggesting that these minerals continue to dissolve along the flow path. The decomposition of anhydrite and gypsum raises the concentration of Ca^{+2} in groundwater, which raises the SI values of calcite and dolomite and may soon precipitate them in the groundwater.

3.4. Multivariate statistical analysis

3.4.1. Correlation analysis

The correlation matrix is an effective statistical tool. It reveals the linear correlation between different physical and chemical variables and the influence of each parameter on the overall hydrochemical data (Figure 11). Two variables are entirely connected if the correlation coefficient (r) values are +1 or −1, which are regarded as a whole correlation coefficient value (Y. Singh & Kumar, 2011). In this study, if (r) is higher than 0.7, it was described as strongly correlated, while 0.4 to 0.7 value is moderately correlated. TDS shows a strong relationship with SO_4^{-2}, TH, Cl^-, $Mg^{+2,}$ and Na^+, suggesting a high contribution of these ions to the groundwater salinity. TH is highly correlated with SO_4^{2-}, $Mg^{+2,}$ and Na^+ and moderately correlated with HCO_3^- and Cl^-, suggesting the temporary hardness predominance (Arumugam, 2010). Cl^- has high correlations with Na^+. Na^+ to Cl-ratio in millimole per liter is equal to 1 if Na^+ and Cl^- are produced entirely from halite disintegration (P. P. Li et al., 2013). In this work, most of the samples are projected below the 1:1 line (Figure 12a). According to (Meybeck, 1987) if the Na^+/Cl^- ratio in water is not 1, silicate weathering is the source of Na^+, but a ratio of about 1 implies halite dissolution. The average Na^+/Cl^- ratio in groundwater samples reported in the current investigation is less than 1:1, indicating that weathering of rocks or human activity may have added to the sodium concentration. NO_3^- has a moderate correlation with Ca^{+2}, and it always indicates contamination from agricultural practice (Sabo and Christopher, 2014). As shown in Figure 12c, Ca^{+2} is positively associated with SO_4^{-2}. More than 75% of the samples are plotted under

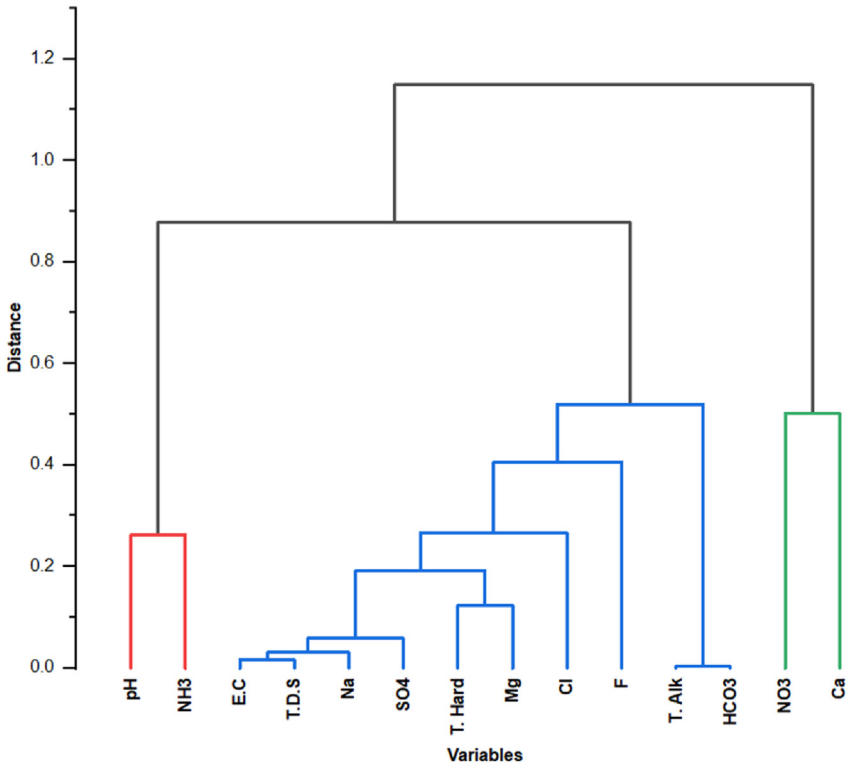

Figure 13. The dendrogram of the chemical variables clusters.

the 2:1 line, which indicates that the calcium in groundwater is not only from calcium sulfate minerals but also from other sources such as weathering of carbonate rocks. Mg^{+2} has a high correlation with SO_4^{-2} and a low with HCO_3^- (Figure 12d), which indicates calcareous magnesium materials which contribute Mg^{+2} and SO_4^{-2} to the groundwater. Carbonate mineral dissolution undoubtedly had a significant role in regional groundwater development, particularly in terms of the origins of Ca^{2+}, Mg^{2+}, and HCO_3^-. If the sources of Ca^{2+} and HCO_3^- can be traced back to carbonate dissolution, the Ca^{2+}/HCO_3^- samples in mmol/L scatter plot should lie between 1:1 and 1:2. In this work, the concentration of

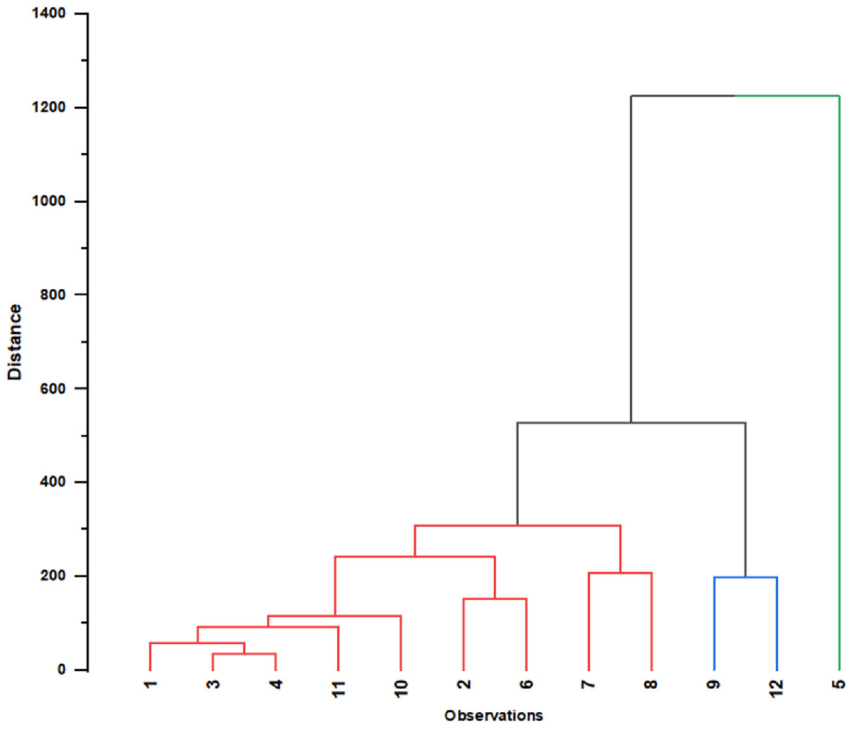

Figure 14. The dendrogram of the sample clusters.

Table 3. Extracted principal components and their total variance.

Parameter	PC 1 (52.52%)	PC 2 (21.86%)	PC 3 (11.72%)
pH	0.09606	−0.33268	**0.53685**
EC	**0.35198**	0.02946	−0.03286
TDS	**0.35344**	0.05078	0.06696
TH	**0.33024**	0.10771	−0.12109
Cl^{-}	**0.30754**	−0.17669	0.2745
F^{-}	**0.247**	−0.18365	−0.31462
SO_4^{-2}	**0.35529**	0.04195	−0.03717
NH_3^{-}	0.07518	−0.31972	**0.54168**
NO_3^{-}	−0.07459	**0.39158**	0.22308
Ca^{+2}	−0.10032	**0.44295**	0.28406
Mg^{+2}	**0.31335**	−0.12771	−0.23247
Na^{+}	**0.36097**	0.01431	−0.003
HCO_3^{-}	0.22527	**0.41359**	0.11369

Ca^{2+} shows a positive trend with HCO_3^{-}. Most samples are plotted below the line of 1:2 (Figure 12/b) demonstrating that carbonate dissolution isn't the primary source of HCO_3^{-}. It can be concluded from correlation analysis that the groundwater in the study area is mainly influenced by mineral dissolution and agricultural practice.

3.4.2. Hierarchical cluster analysis (HCA)

HCA can potentially classify groundwater samples into different water quality groups or hydrochemical facies (Daughney et al., 2012). HCA applies the Euclidean separation technique as a similarity measure to distinguish between groundwater samples based on their hydrochemical characteristics. The dendrogram in Figure 13 obtained for chemical parameters showed three clusters (C1, C2, and C3). Due to the role of the sampling sites in the establishment of clusters, Water sample sites that are geographically close are mostly in the same cluster. C1 includes pH and NH_3^{-} with a high degree of similarity (77%). The occurrence of NH_3^{-} in groundwater results from the degradation of the organic materials by bacteria (X. X. Li et al., 2013); therefore, in this study, the first cluster might indicate anthropogenic contamination such as seepage from septic tanks. This cluster may also reflect the effect of organic pollution on the pH of the groundwater. C2 involves EC, TDS, Na^{+}, SO_4^{-2}, TH, Cl^{-}, F^{-}, HCO_3^{-}, Mg^{+2}. The salinity of groundwater is mostly influenced by these parameters. This cluster could possibly show the effect of rock-water interaction on groundwater samples (Sharma et al., 2022). C3 includes NO_3^{-} and Ca^{+2}. A high concentration of NO_3^{-} is due to irrigation return flow (Nethononda et al., 2019). The main source of Ca^{+2} in groundwater in the study area is the dissolution of carbonate rocks, as suggested by the interionic interactions. Thus, the parameters in the third cluster may indicate carbonate weathering and agricultural contamination (Sabo and Christopher, 2014). The dendrogram of Figure 14 illustrates the general clustering of the groundwater samples in the study area. According to their chemical compositions, groundwater samples are clustered into three groups. The first group includes sample locations of 1,2,3,4,6,7,8,10,11, the second cluster is 9,12, and the third cluster is sample number 5. The samples of the first cluster are associated with low chemical contents, and the maximum values of the parameters are below the standard prescribed by WHO (Edition, 2011). Groundwater samples of cluster 2 have higher chemical content than cluster 1, and some parameters exceed the permissible limit. Samples in cluster 3 are considered highly mineralized due to the high values of many parameters such as TDS and Na^{+}. According to Piper and Chadha diagrams, the groundwater samples in C1 are of Ca–Mg– HCO_3 water, C2 represented in Na–HCO_3 water type, and C3 is Na–Cl water type. The geochemistry of C2 and C3 show high similarity as they are projected near to each other in the hydrochemical plots. Groundwater quality varies smoothly throughout the region, as evidenced by the spatial distribution of the clustered samples. This variation could be attributed to the equally dominant hydrogeological environment in the study area.

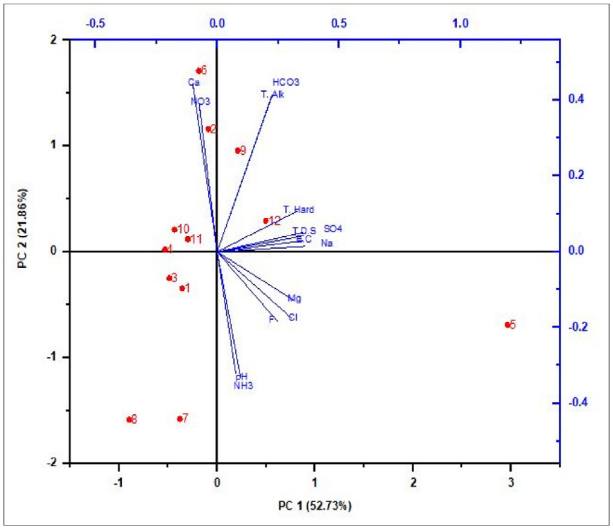

Figure 15. Biplot of PC 1 versus PC 2.

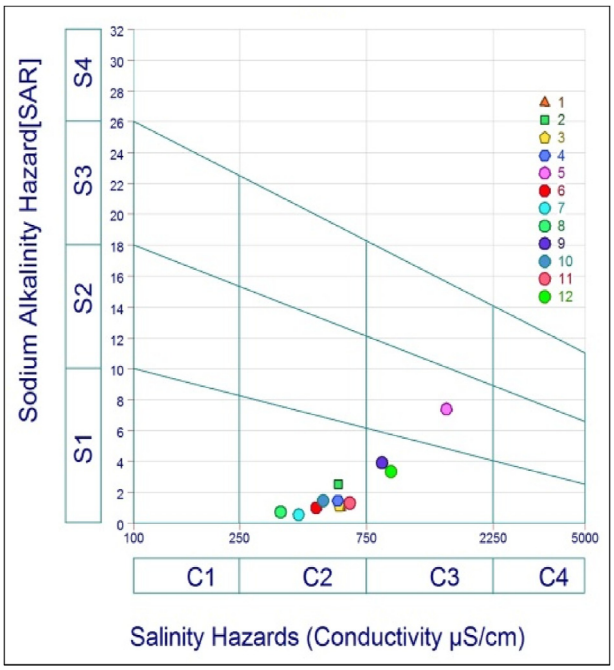

Figure 16. The USSL diagram.

3.4.3. Principal component analysis (PCA)

PCA is a pattern recognition method that reduces data dimensionality to facilitate visualization and analysis. The extracted principal components are orthogonal to one another. 12 PCs were extracted in this study, but only PCs with eigenvalues greater than one were selected. In this study, according to (C. W. Liu et al., 2003), variables loading higher than 0.3 are considered for the interpretation of the result as they strongly influence the principal component. Table 3 shows the results of the PCA based on the correlation matrix between the chemical and physical components. In this study, three PCs were extracted, describing 86.1% of total variances. PC1 accounted for most of the total variance (52.52%) and is associated with high loading of EC, TDS, TH, Cl^{-}, F^{-}, SO_4^{-2}, Mg^{+2}, and Na^{+}. PC1 contains the major cations and anions that seem to be

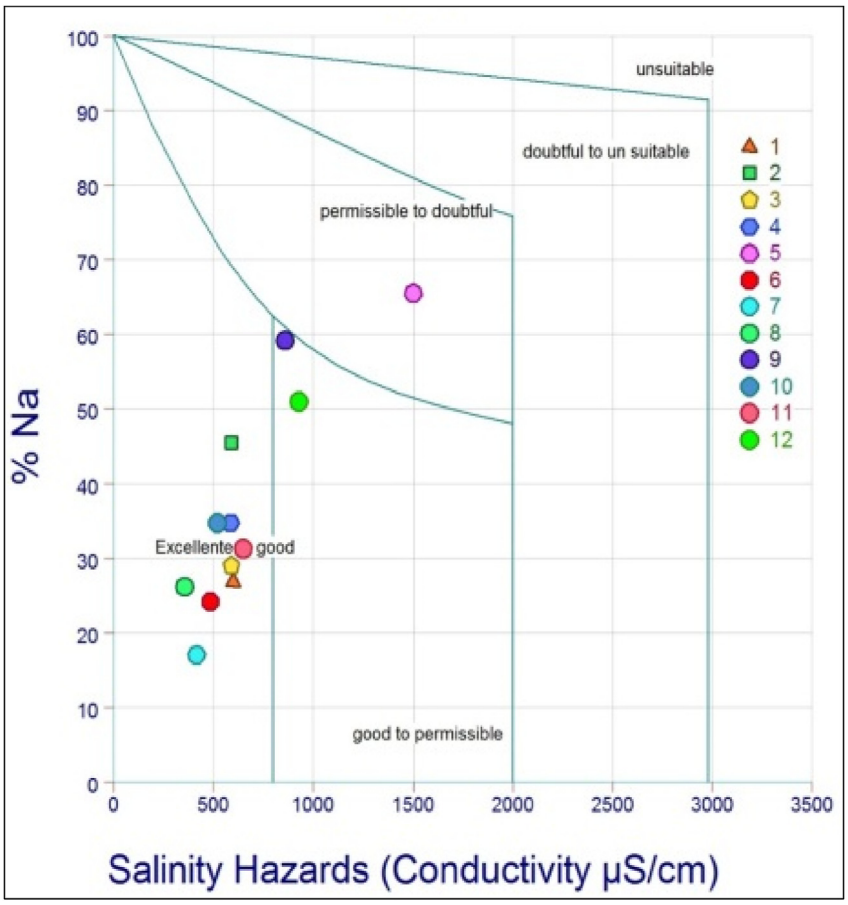

Figure 17. Wilcox diagram.

related to the dissolution of the geological component from rock-water interaction. This was also interpreted by (Gopinath et al., 2018). This PC depicts the second cluster of HCA and suggests that high values of TDS are affected by Na^{+}, Cl^{-}, Mg^{+2}, SO_4^{-2}, and F^{-} (P. Liu et al., 2017). suggested that the strong positive PC coefficient of Mg^{+2} and Ca^{+2} indicates that these ions are derived from weathering of carbonate minerals. This component also represented the salinity of water since TDS, Na^{+}, and Cl^{-} showed the highest loading as the main cause of salinization. The concentration of F^{-} is relatively low, which contributed less to salinity. PC2 accounted for 21.86% of variance and is associated with medium to high positive loading of NO_3^{-}, Ca^{+2} and HCO_3^{-}. The presence of NO_3^{-} in groundwater suggests contamination from agricultural activities. High coefficients of and NO_3^{-} are due to infiltration of wastewater and irrigation return flow (Nethononda et al., 2019). PC2 may also indicate carbonate dissolution. PC3 shows high positive loading of pH and NH_3^{-} and accounted for 11.72% of the total variance. PC3 suggests that the pH of groundwater is influenced by NH_3^{-}. This component represents the in the influence of anthropogenic activities such as organic contamination on the pH of water and it reflects C1 of HCA. Figure 15 shows the biplot of PC1 (52.52% variance) versus PC2 (21.86% variance), which illustrates the orientation of different parameters towards the plotted components and the influence of the two components on the groundwater samples. The chemical variables in the PC1 effects three water samples in this study: samples 9, 12, and 5. These samples are highly mineralized and influenced by the minerals dissolution process. Samples 1, 2, 6, 10, and 11 are impacted by PC2 while the remaining samples fall in the transition zone, which means they are controlled by ions in the PC1 and PC2, simultaneously. According to the principal component analysis, the water chemistry in the study area is mostly influenced by mineral dissolution and anthropogenic activities such as agricultural practices and septic tank.

3.5. Irrigation indices

Groundwater is mostly used for agricultural purposes in the Bahri area since farming is the principal profession of the residents. On the other hand, irrigation water poses the greatest harm to the groundwater quality in the study area. The quality of the irrigation water is determined by the concentration of dissolved sodium relative to the other major cations and the presence of toxic elements in the groundwater. The incorporation of Na^{+} into clay particles accelerates the base-exchange process by eliminating Ca^{+2} and Mg^{+2} ions. Sodium adsorption ratio (SAR) and sodium percent (Na^{+}%) are employed in this study to assess the appropriateness of groundwater for irrigation. SAR is the most widely used index to assess groundwater quality for irrigation. The sodium concentration is one of the major components in evaluating water quality for irrigation since high sodium concentration potentially affects soil permeability (Sadashivaiah et al., 2008). The soil becomes unusable for agriculture after prolonged exposure to groundwater with a high content of Na^{+}(Younger and Casey, 2003). Figure 16 shows the United States salinity laboratory (USSL) diagram (Richards, 1954), which takes the EC of the water samples as the main component for evaluation. EC is typically regarded as a crucial factor in understanding whether water is suitable for irrigation purposes. Any water's EC is dependent on the amount of salts present, which in turn has an impact on crop production. In this study, the values of SAR range from 0.56 to 7.42. About 75% of the samples fell under the excellent category with low sodium and salinity hazard. This category can be used safely for crop irrigation. 16.6% of the samples fell under the C3S1 class with low alkali, and medium salinity hazard and 8.3% of the samples represented the good category and plotted in C3S2 class. The C2S1, C3S1, and C3S2 classes respectively reflect Cluster 1, Cluster 2, and Cluster 3 obtained from hierarchical cluster analysis.

Na^+ % index is widely used to indicate sodium hazards. High Na^+ concentration reduces the soil permeability and, thus, reduces the capacity of the water movement (Ayers et al., 1985). Alkaline soils are formed when Na^+ reacts with HCO_3, whereas saline soils are formed when Na^+ reacts with Cl^-. The observed Na^+% ranges from 17 to 65.6. Wilcox's (1948) diagram in Figure 17 relates EC to Na^+ % to categorize the groundwater samples. In the present work, 75% of the water samples are plotted in the excellent category, 16.66% are located in the good to permissible class, and 8.33% are projected in the permissible to doubtful class. The doubtfulness is due to the high salinity in the groundwater samples. As in SAR, the categories of Na^+ % can be read in the light of the hierarchical cluster analysis. The groundwater in the study area is suitable for irrigation, and no threats to soil structure and crop yield are posed. However, two samples (5 and 9) are associated with high salinity, and the ongoing use of these samples in irrigation may induce salinity hazards.

4. Conclusions

The study evaluated the quality of the groundwater for domestic and agricultural usage in north Bahri city, Sudan, using hydrochemical and multivariate statistical methods. The main conclusions are summarized:

- The primary hydrochemical analysis for the measured parameters demonstrated that the composition of the groundwater is fresh to alkaline. The spatial distribution of major ions except for Ca^{+2} and HCO_3 showed that the water samples in the eastern part are highly mineralized compared to the west. This reflects the chemical nature of the Nile River, which considers the main source of recharge.
- Hydrochemical plots such as Piper, Chadha, and Durov diagrams revealed the dominant groundwater facies. Ca–Mg–HCO_3 water type is prevailing, followed by Na–HCO_3 and Na–Cl water types.
- Based Gibbs plot, mineral dissolution and precipitation are the main natural factors influencing the groundwater chemistry in the study area. The mineral content of anhydrite, dolomite, aragonite, calcite, gypsum, and halite was calculated using saturation indices (SI). SI indicated the precipitation of aragonite, calcite, and dolomite in 41.6%, 58.33%, and 75% of groundwater samples, respectively.
- Multivariate statistical techniques have been demonstrated to be an effective tool in groundwater quality assessment. Correlation analysis is applied to identify the interrelationship between the measured variables and the role of each variable on the overall quality. HCA has been used to group the major ions and groundwater samples based on their physiochemical similarities. The clustering for major ions reveals two factors controlling water quality: mineral dissolution and to less degree, anthropogenic activities. Additionally, sample clustering classifies groundwater into three groups as low, medium, and highly mineralized groundwater. Three Principal components (PCs) explained 86.1 % of the total variance, indicating that groundwater quality is affected by water-rock interaction, agricultural practice, and septic tanks.
- Sodium adsorption ratio (SAR) and sodium percent (Na^+%) were utilized to assess the irrigation compatibility of groundwater. According to USSL and Wilcox diagrams, more than 75% of groundwater samples are excellent for irrigation.
- The integrated approaches proved to be robust and efficient in highlighting and evaluating groundwater quality characteristics in the north Bahri locality. This study recommended the installation of groundwater quality monitoring scheme to ensure water supply sustainability.

Declarations

Author contribution statement

Musaab A.A. Mohammed: Conceived and designed the experiments; Performed the experiments; Analyzed and interpreted the data; Contributed reagents, materials, analysis tools or data; Wrote the paper.

Norbert P. Szabo; Péter Szűcs: Analyzed and interpreted the data; Contributed reagents, materials, analysis tools or data; Wrote the paper.

Funding statement

This research did not receive any specific grant from funding agencies in the public, commercial, or not-for-profit sectors.

Data availability statement

Data included in article/supp. material/referenced in article.

Declaration of interest's statement

The authors declare no conflict of interest.

Additional information

No additional information is available for this paper.

Acknowledgements

The authors would like to thank Khartoum State water corporation (KSWC) and the general directorate of groundwater and wadies for their support during the laboratory analysis. The authors also are thankful to Mr. Mohammed Eid, PhD student, Department of Hydrogeology, University of Miskolc, for his help during the hydrochemical analysis.

References

Abdelaziz, S., Gad, M.I., El Tahan, A.H.M.H., 2020. Groundwater quality index based on PCA: wadi El-Natrun, Egypt. J. Afr. Earth Sci. 172, 103964.
Abdelsalam, Y.E., Ea, E.M., Elhadi, H. El., 2016. Problems and factors which retard the development and the utilization of groundwater for drinking purposes in the Khartoum state-Sudan. In: 7th International Conference on Environment and Engineering Geophysics & Summit Forum of Chinese Academy of Engineering on Engineering Science and Technology, pp. 449–451.
Abdo, G., Salih, A., 2012. Challenges Facing Groundwater Management in Sudan.
Adams, S., Titus, R., Pietersen, K., Tredoux, G., Harris, C., 2001. Hydrochemical characteristics of aquifers near sutherland in the western Karoo, South Africa. J. Hydrol. 241 (1–2), 91–103.
Adimalla, N., 2019. Groundwater quality for drinking and irrigation purposes and potential health risks assessment: a case study from semi-arid region of South India. Expos. Heal. 11 (2), 109–123.
Alsidig, H.E., Al-Hagaz, Y.A., 2019. Hydro-chemical Characteristics and Groundwater Quality in the East Nile Area. Khartoum State, Sudan.
Appelo, C.A.J., Postma, D., 2005. Geochemistry, Groundwater and Pollution, 2nd. Balkema, Rotterdam.
Arumugam, K., 2010. Assessment of Groundwater Quality in Tirupur Region.
Asadi, E., Isazadeh, M., Samadianfard, S., Ramli, M.F., Mosavi, A., Nabipour, N., Shamshirband, S., Hajnal, E., Chau, K.-W., 2020. Groundwater quality assessment for sustainable drinking and irrigation. Sustainability 12 (1), 177.
Awad, A.Z., 1994. Stratigraphic Palyloical and Paleoclogical Studies in East Central Sudan (Khartoum–Kosti Basin) Late Jurassic to Mid Tertiary. Berliner Geowiss B161Technical univ Berliner.
Ayers, R.S., Westcot, D.W., others, 1985. Water Quality for Agriculture, 29. Food and Agriculture Organization of the United Nations Rome.
Behera, B., Das, M., 2018. Application of multivariate statistical techniques for the characterization of groundwater quality of Bacheli and Kirandul area, Dantewada district, Chattisgarh. J. Geol. Soc. India 91 (1), 76–80.
Ben Brahim, F., Bougharriou, E., Bouri, S., 2021. Multicriteria-analysis of deep groundwater quality using WQI and fuzzy logic tool in GIS: a case study of Kebilli region, SW Tunisia. J. Afr. Earth Sci. 180 (April), 104224.
Bhakar, P., Singh, A.P., 2019. Groundwater quality assessment in a hyper-arid region of Rajasthan, India. Nat. Res. Res. 28 (2), 505–522.
Bhimanagouda, B.P.V., Pinto, S.M., Thejashree, G., Shivakumar, H.V., Vignesh, B., Nanjappa, K.L., 2020. Multivariate statistics and water quality index (WQI) approach for geochemical assessment of groundwater quality—a case study of Kanavi Halla Sub-Basin, Belagavi, India. Environ. Geochem. Heal. 42 (9), 2667–2684.
Boateng, T.K., Opoku, F., Acquaah, S.O., Akoto, O., 2016. Groundwater quality assessment using statistical approach and water quality index in Ejisu-Juaben Municipality, Ghana. Environ. Earth Sci. 75 (6), 1–14.
Chadha, D.K., 1999. A proposed new diagram for geochemical classification of natural waters and interpretation of chemical data. Hydrogeol. J. 7 (5), 431–439.
Daughney, C.J., Raiber, M., Moreau-Fournier, M., Morgenstern, U., van der Raaij, R., 2012. Use of hierarchical cluster analysis to assess the representativeness of a baseline groundwater quality monitoring network: comparison of New Zealand's

national and regional groundwater monitoring programs. Hydrogeol. J. 20 (1), 185–200.
Dlamini, A.E., Demlie, M., 2020. Integrated hydrogeological, hydrochemical and environmental isotope investigation of the area around the Kusile Power Station, Mpumalanga, South Africa. J. Afr. Earth Sci. 172, 103958.
Duan, R., Li, P., Wang, L., He, X., Zhang, L., 2022. Hydrochemical characteristics, hydrochemical processes and recharge sources of the geothermal systems in Lanzhou City, northwestern China. Urban Climate 43 (126), 101152.
Durov, S.A., 1948. Natural waters and graphic representation of their composition. Dokl Akad Nauk SSSR 59 (3), 87–90.
Edition, F., 2011. Guidelines for drinking-water quality. WHO Chronicle 38 (4), 104–108.
Elkrail, A., Shu, L., Kheir, O., Zhenchun, H., 2003. Hydrchemical Evaluation of Groundwater in Khartoum State.
Elumalai, V., Nethononda, V.G., Manivannan, V., Rajmohan, N., Li, P., Elango, L., 2020. Groundwater quality assessment and application of multivariate statistical analysis in Luvuvhu catchment, Limpopo, South Africa. J. Afr. Earth Sci. 171, 103967.
Enyegue A Nyam, F.M., Yomba, A.E., Tchikangoua, A.N., Bounoung, C.P., Nouayou, R., 2020. Assessment and characterization of groundwater quality under domestic distribution using hydrochemical and multivariate statistical methods in Bafia, Cameroon. Groundwater for Sustain. Develop. 10, 100347.
Farah, E.A., Abdullatif, O.M., Kheir, O.M., Barazi, N., 1997. Groundwater resources in a semi-arid area: a case study from central Sudan. J. Afr. Earth Sci. 25 (3), 453–466.
Farah, E.A., Mustafa, E.M.A., Kumai, H., 2000. Sources of groundwater recharge at the confluence of the Niles, Sudan. Environ. Geol. 39 (6), 667–672.
Gibbs, R.J., 1970. Mechanisms controlling world water chemistry. Science 170 (3962), 1088–1090.
Gopinath, S., Srinivasamoorthy, K., Vasanthavigar, M., Saravanan, K., Prakash, R., Suma, C.S., Senthilnathan, D., 2018. Hydrochemical characteristics and salinity of groundwater in parts of nagapattinam district of Tamil nadu and the union territory of puducherry, India. Carbon. Evap. 33 (1), 1–13.
Gulgundi, M.S., Shetty, A., 2018. Groundwater quality assessment of urban Bengaluru using multivariate statistical techniques. Appl. Water Sci. 8 (1), 1–15.
Hailu, Y., Tilahun, E., Brhane, A., Resky, H., Sahu, O., 2019. Ion exchanges process for calcium, magnesium and total hardness from ground water with natural zeolite. Groundwater for Sustain. Develop. 8, 457–467.
Hassan, I., Elhassan, B.M., Mustafa, M.A., 2017. Heavy metals and refractory organic compounds in Khartoum state's groundwater resources. Europ. J. Eng. Technol. Res. 2 (8), 13–16.
Hem, J.D., 1985. Study and Interpretation of the Chemical Characteristics of Natural Water, 2254. Department of the Interior, US Geological Survey.
Ibrahim, R.G.M., Korany, E.A., Tempel, R.N., Gomaa, M.A., 2019. Processes of water–rock interactions and their impacts upon the groundwater composition in Assiut area, Egypt: applications of hydrogeochemical and multivariate analysis. J. Afr. Earth Sci. 149, 72–83.
Ismail, E., Abdelhalim, A., Heleika, M.A., 2021. Hydrochemical characteristics and quality assessment of groundwater aquifers northwest of Assiut district, Egypt. J. Afr. Earth Sci. 181, 104260.
Kaur, L., Rishi, M.S., Arora, N.K., 2021. Deciphering pollution vulnerability zones of River Yamuna in relation to existing land use land cover in Panipat, Haryana, India. Environ. Monitor. Assess. 193 (3).
Kaur, L., Rishi, M.S., Sharma, S., Sharma, B., Lata, R., Singh, G., 2019. Hydrogeochemical characterization of groundwater in alluvial plains of river Yamuna in northern India: an insight of controlling processes. J. King Saud Univ. Sci. 31 (4), 1245–1253.
Kaur, L., Rishi, M.S., Siddiqui, A.U., 2020. Deterministic and probabilistic health risk assessment techniques to evaluate non-carcinogenic human health risk (NHHR) due to fluoride and nitrate in groundwater of Panipat, Haryana, India. Environ. Poll. 259, 113711.
Khalid, S., 2019. An assessment of groundwater quality for irrigation and drinking purposes around brick kilns in three districts of Balochistan province, Pakistan, through water quality index and multivariate statistical approaches. J. Geochem. Exploration 197, 14–26.
Kheiralla, M.k., 1966. Study of the Nubian Sand Stone Formation of the Nile Vally between 14 N and 17 42 N, with Reference to Groundwater Geology. University of Khartoum.
Khodapanah, L., Sulaiman, W.N.A., Khodapanah, N., 2009. Groundwater quality assessment for different purposes in Eshtehard District, Tehran, Iran. Europ. J. Scient. Res. 36 (4), 543–553.
Kudoda, A.M., Abdalla, O.A.E., 2015. Hydrochemical characterization of the main aquifers in Khartoum, the capital city of Sudan. Environ. Earth Sci. 74 (6), 4771–4786.
Kumar, P.J.S., Jegathambal, P., James, E.J., 2011. Multivariate and geostatistical analysis of groundwater quality in palar river basin. Int. J. Geol. 5 (4), 12. https://www.researchgate.net/publication/216216488.
Li, P., Qian, H., Wu, J., 2018a. Conjunctive use of groundwater and surface water to reduce soil salinization in the Yinchuan Plain, North-West China. Int. J.Water Res. Develop. 34 (3), 337–353.
Li, P., Tian, R., Liu, R., 2019. Solute geochemistry and multivariate analysis of water quality in the guohua phosphorite mine, guizhou province, China. Exposure and Health 11 (2), 81–94.
Li, P., Wu, J., Qian, H., 2013. Assessment of groundwater quality for irrigation purposes and identification of hydrogeochemical evolution mechanisms in Pengyang County, China. Environ. Earth Sci. 69 (7), 2211–2225.
Li, P., Wu, J., Qian, H., 2016. Hydrochemical appraisal of groundwater quality for drinking and irrigation purposes and the major influencing factors: a case study in and around Hua County, China. Arab. J. Geosci. 9 (1), 1–17.
Li, P., Wu, J., Tian, R., He, S., He, X., Xue, C., Zhang, K., 2018b. Geochemistry, hydraulic connectivity and quality appraisal of multilayered groundwater in the Hongdunzi Coal Mine, Northwest China. Mine Water and the Environ. 37 (2), 222–237.
Li, X., Chu, Z., Liu, Y., Zhu, M., Yang, L., Zhang, J., 2013. Molecular characterization of microbial populations in full-scale biofilters treating iron, manganese and ammonia containing groundwater in Harbin, China. Biores. Technol. 147, 234–239.
Liu, C.W., Lin, K.H., Kuo, Y.M., 2003. Application of factor analysis in the assessment of groundwater quality in a Blackfoot disease area in Taiwan. Sci. Total Environ. 313 (1–3), 77–89.
Liu, P., Hoth, N., Drebenstedt, C., Sun, Y., Xu, Z., 2017. Hydro-geochemical paths of multi-layer groundwater system in coal mining regions—using multivariate statistics and geochemical modeling approaches. Sci. Total Environ. 601, 1–14.
Lloyd, J.W., Heathcote, J.A.A., 1985. Natural Inorganic Hydrochemistry in Relation to Ground Water.
Lu, K.L., Liu, C.W., Jang, C.S., 2012. Using multivariate statistical methods to assess the groundwater quality in an arsenic-contaminated area of Southwestern Taiwan. Environ. Monitor. Assess. 184 (10), 6071–6085.
Ma, R., Shi, J., Liu, J., Gui, C., 2014. Combined use of multivariate statistical analysis and hydrochemical analysis for groundwater quality evolution: a case study in north chain plain. J. Earth Sci. 25 (3), 587–597.
Masoud, A.M., Ali, M.H., 2020. Coupled multivariate statistical analysis and WQI approaches for groundwater quality assessment in Wadi El-Assiuty downstream area, Eastern Desert, Egypt. J. Afr. Earth Sci. 172, 103982.
Meybeck, M., 1987. Global chemical weathering of surficial rocks estimated from river dissolved loads. Am. J. Sci. 287 (5), 401–428.
Nethononda, V.G., Elumalai, V., Rajmohan, N., 2019. Irrigation return flow induced mineral weathering and ion exchange reactions in the aquifer, Luvuvhu catchment, South Africa. J. Afr. Earth Sci. 149, 517–528.
Osiakwan, G.M., Appiah-Adjei, E.K., Kabo-Bah, A.T., Gibrilla, A., Anornu, G., 2021. Assessment of groundwater quality and the controlling factors in coastal aquifers of Ghana: an integrated statistical, geostatistical and hydrogeochemical approach. J. Afr. Earth Sci. 184, 104371.
Othman, A., Ibraheem, I.M., Ghazala, H., Mesbah, H., Dahlin, T., 2019. Hydrogeophysical and hydrochemical characteristics of Pliocene groundwater aquifer at the area northwest El Sadat city, West Nile Delta, Egypt. J. Afr. Earth Sci. 150, 1–11.
Piper, A.M., 1944. A graphic procedure in the geochemical interpretation of water-analyses. Eos, Transact. Am. Geophysical Union 25 (6), 914–928.
Rafaâ Trigui, M., Trabelsi, R., Zouari, K., Agoun, A., 2021. Implication of hydrogeological and hydrodynamic setting on water quality of the Complex Terminal Aquifer in Kebili (southern Tunisia): the use of geochemical indicators and modelling. J. Afr. Earth Sci. 176.
Rafique, T., Naseem, S., Ozsvath, D., Hussain, R., Bhanger, M.I., Usmani, T.H., 2015. Geochemical controls of high fluoride groundwater in Umarkot sub-district, Thar Desert, Pakistan. Sci. Total Environ. 530, 271–278.
Ren, X., Li, P., He, X., Su, F., Elumalai, V., 2021. Hydrogeochemical processes affecting groundwater chemistry in the central part of the guanzhong basin, China. Archiv. Environ. Contamin. Toxicol. 80 (1), 74–91.
Richards, L.A., 1954. Diagnosis and improvement of saline and alkali soils. LWW 78 (2).
Rishi, M.S., Kaur, L., Sharma, S., 2020. Groundwater quality appraisal for non-carcinogenic human health risks and irrigation purposes in a part of Yamuna sub-basin, India. Human and Ecol. Risk Assess. 26 (10), 2716–2736.
Sabo, A., Christopher, E.O., 2014. Physicochemical and bacteriological quality of ground water at abubakar tatari Ali polytechnic Bauchi, Nigeria. Europ. Scientif. J. 10 (18).
Sadashivaiah, C., Ramakrishnaiah, C.R., Ranganna, G., 2008. Hydrochemical analysis and evaluation of groundwater quality in Tumkur Taluk, Karnataka State, India. Int. J. Environ. Res. Public Heal. 5 (3), 158–164.
Saeed, E.M., 1974. Geological and Hydrogeological Studies of Khartoum Province, Sudan. PhD Thesis. Cairo Univ.
Sharma, T., Bajwa, B.S., Kaur, I., 2022. Hydro-geochemical characteristics and quality appraisal of aquifers using multivariate statistics and associated risk assessment in Tarn-Taran district, Punjab, India. Environ. Sci. Poll. Res. 1–23.
Sheikhi, S., Faraji, Z., Aslani, H., 2021. Arsenic health risk assessment and the evaluation of groundwater quality using GWQI and multivariate statistical analysis in rural areas, Hashtroud, Iran. Environ. Sci. Poll. Res. 28 (3), 3617–3631.
Shrestha, S., Kazama, F., 2007. Assessment of surface water quality using multivariate statistical techniques: a case study of the Fuji river basin, Japan. Environ. Model. Software 22 (4), 464–475.
Singh, S.P., Tripathi, S.K., Vimal, K., Ashok, K., Priyankar, R., others, 2015. Hydrochemical investigation and groundwater quality evolution for irrigation purpose in some blocks of Varanasi district, Uttar Pradesh, India. Int. J. Trop. Agricul. 33 (2), 1653–1660 (Part IV)).
Singh, Y., Kumar, M., 2011. Application of statistical methods to analyze groundwater quality. J. Earth Sci. Geotechnical Eng. 1 (1), 1792–9660.
Sunkari, E.D., Abu, M., Zango, M.S., Wani, A.M.L., 2020. Hydrogeochemical characterization and assessment of groundwater quality in the Kwahu-Bombouaka group of the Voltaian supergroup, Ghana. J. Afr. Earth Sci. 169, 103899.
Todd, D.K., Mays, L.W., 2004. Groundwater Hydrology. John Wiley \& Sons.
Whiteman, A.J., 1971. Geology of the Sudan Republic.
Wilcox, L.V., 1948. The Quality of Water for Irrigation Use.
Wu, J., Li, P., Qian, H., Duan, Z., Zhang, X., 2014. Using correlation and multivariate statistical analysis to identify hydrogeochemical processes affecting the major ion chemistry of waters: a case study in Laoheba phosphorite mine in Sichuan, China. Arab. J. Geosciences 7 (10), 3973–3982.
Wu, J., Li, P., Wang, D., Ren, X., Wei, M., 2020. Statistical and multivariate statistical techniques to trace the sources and affecting factors of groundwater pollution in a

rapidly growing city on the Chinese Loess Plateau. Human and Ecol. Risk Assess. 26 (6), 1603–1621.
Yadav, K.K., Gupta, N., Kumar, V., Choudhary, P., Khan, S.A., 2018. GIS-based evaluation of groundwater geochemistry and statistical determination of the fate of contaminants in shallow aquifers from different functional areas of Agra city, India: levels and spatial distributions. RSC Adv. 8 (29), 15876–15889.
Yidana, S.M., Bawoyobie, P., Sakyi, P., Fynn, O.F., 2018. Evolutionary analysis of groundwater flow: application of multivariate statistical analysis to hydrochemical data in the Densu Basin, Ghana. J. Afr. Earth Sci. 138, 167–176.
Younger, P., Casey, V., 2003. A simple method for determining the suitability of brackish groundwaters for irrigation. Waterlines 11–13.
Zhang, Y., Li, X., Luo, M., Wei, C., Huang, X., Xiao, Y., Qin, L., Pei, Q., 2021. Hydrochemistry and entropy-based groundwater quality assessment in the suining area, southwestern China. J. Chem.
Ziani, S., Khattach, D., Abderbi, J., Nouayti, N., Makkaoui, M., 2021. Assessment of groundwater quality using statistical methods in the Isly basin (Horst Belt, Morocco). E3S Web of Conf. 240, 1–4.